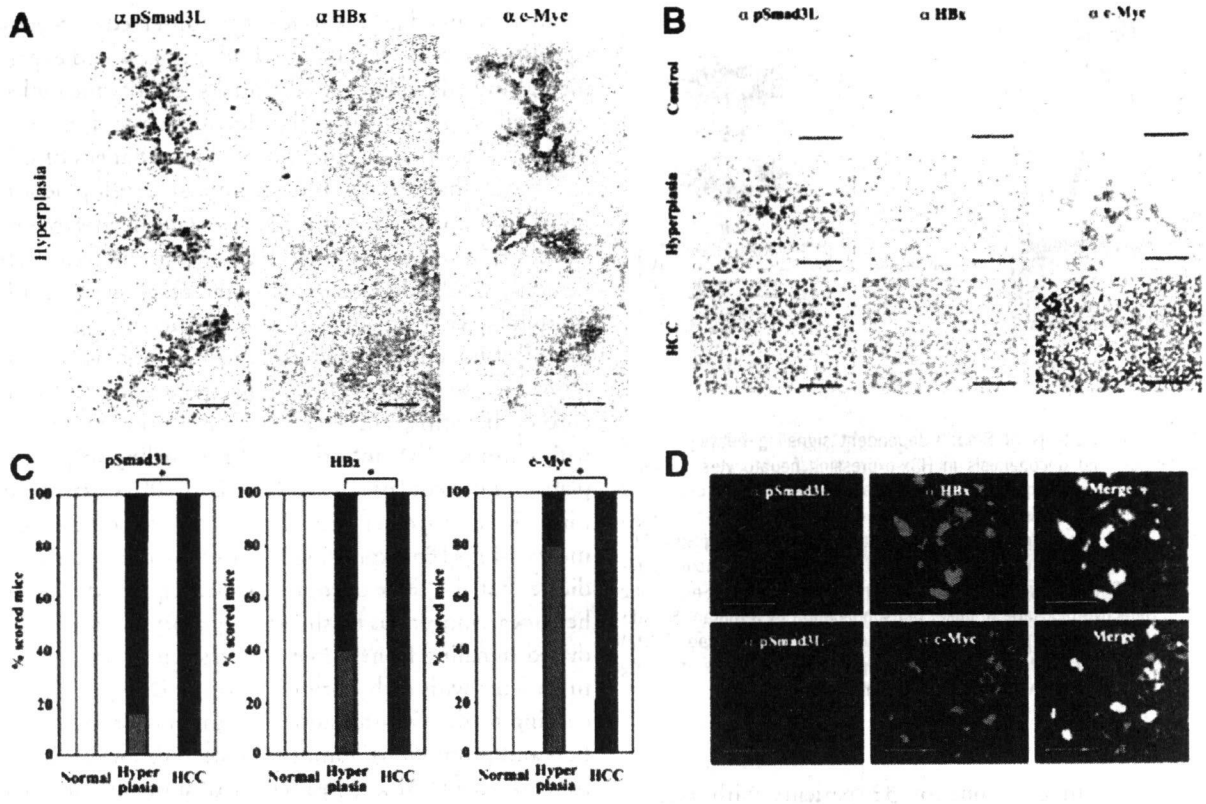

Fig. 6. The pSmad3L/c-Myc pathway was activated as HBx transgenic mouse liver progressed through hyperplasia to HCC. (A) Distribution of pSmad3L, HBx, and c-Myc in hyperplastic specimens from HBx transgenic mouse liver. (B) Distributions of pSmad3L, HBx, and c-Myc in normal liver, hyperplasia, and HCC specimens from HBx transgenic mice. Immunostaining for pSmad3L, HBx, and c-Myc was present in hyperplastic hepatocytes surrounding central veins in HBx transgenic mouse liver [(A) and (B), hyperplasia panels], and was distributed diffusely in HCC specimens [(B), HCC panel]. All sections were counterstained with hemotoxylin (blue). Brown color indicates specific Ab reactivity. Bar = 50 μm. (C) Hepatocytic pSmad3L, HBx, and c-Myc increased as HBx transgenic mouse liver progressed from hyperplasia to HCC. Staining for pSmad3L, HBx, and c-Myc was detected minimally in normal mouse livers, but was strongly up-regulated in neoplastic livers. In HCC, pSmad3L, HBx, and c-Myc were significantly greater than in livers with hyperplasia. *$P < 0.05$. Extent of pSmad3L, HBx, and c-Myc: □, 0; ⌊⌋, 1; ⌊_, 2; ■, 3; ■, 4. (D) Hepatocytic pSmad3L in hyperplastic specimens from HBx transgenic mouse liver was colocalized with HBx and c-Myc. Hyperplasia sections of HBx transgenic mouse livers were stained for immunofluorescence to simultaneously detect pSmad3L (red) and HBx or c-Myc (green). Yellow color indicates overlap of proteins. Hepatocytes immunoreactive for pSmad3L showed colocalization of HBx (upper column) and c-Myc (lower column). Bar = 50 μm.

of HCC.[32] In contrast, HCC occasionally develops in healthy HBV surface antigen carriers, who are persistently infected with HBV but have normal liver function parameters and no necroinflammation.[33] This indicates that HBV itself has a direct influence on hepatocarcinogenesis in early chronic hepatitis B. Although integration of the viral genome into chromosomal DNA has not been reported in patients with HCV infection, integration of HBV has been detected in almost all cases of chronic hepatitis B,[3] leading to activation of the HBx-mediated oncogenic pathway.[4] It is noteworthy that HCC developed in patient 10 (Table 2), who showed strong pSmad3L positivity of hepatocytic nuclei but had minimal necroinflammatory activity (A1) or fibrosis (F1). In summary, HCV contributes indirectly to the development of HCC through chronic inflammation in early chronic hepatitis C. In contrast, HBV directly triggers the JNK/pSmad3L oncogenic pathway in early chronic hepatitis B, thus playing a role beyond mere stimulation of the host immune response.

Our findings also open up a new avenue to understanding the development and progression of hepatic fibrogenesis.[34] Whereas HSCs have traditionally been considered as the principal source of liver fibrosis, mature hepatocytes can acquire a mesencymal phenotype and perform the functions of activated HSC—that is, they can contribute to fibrogenesis.[35,36] In support of this notion, pSmad3L-mediated signaling promotes liver fibrosis by hepatocytes as well as activated HSCs during long-standing carcinogenesis.[13,18,20] In this manner, either HBV- or HCV-related chronic hepatitis progresses through fibrogenesis to HCC.

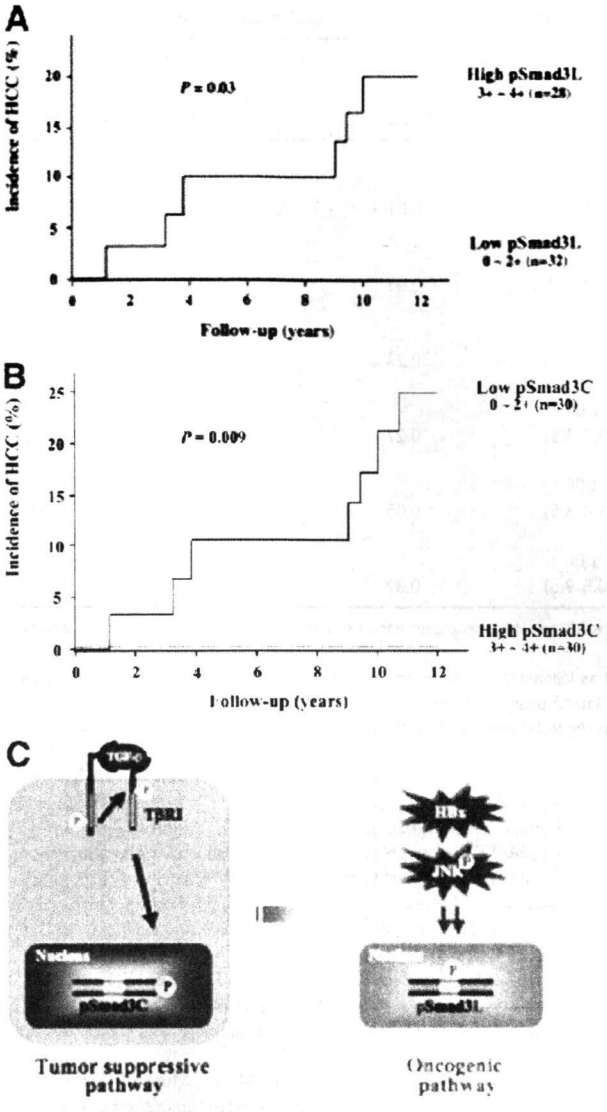

Fig. 7. Chronic hepatitis B patients with hepatocytes positive for pSmad3L and negative for pSmad3C increased risk of HCC development. (A) HCC occurred subsequently among patients whose hepatocytes in chronic hepatitis B specimens were strongly positive for pSmad3L. Incidence of HCC was significantly higher in patients with abundant Smad3L phosphorylation (scores 3 to 4, solid line) in hepatocytic nuclei versus those with sparse Smad3L phosphorylation (scores 0 to 2, dotted line). (B) HCC did not occur subsequently among patients whose hepatocytes in chronic hepatitis B specimens were strongly positive for pSmad3C. HCC occurred only in patients with sparse Smad3C phosphorylation (scores 0 to 2, solid line) in hepatocytic nuclei, while no patients with abundant Smad3C phosphorylation (scores 3 to 4, dotted line) have developed HCC. Cumulative rates of HCC occurrence from chronic hepatitis B were compared between cases with high and low phosphorylation of Smad3L and Smad3C (Kaplan-Meier analysis and log-rank test). (C) HBx protein shifted hepatic TGF-β signaling from the tumor-suppressive pSmad3C pathway to the oncogenic JNK-dependent pSmad3L pathway in early stages of chronic hepatitis B. Normal hepatocytes exhibited TGF-β–dependent Smad3 phosphorylation at the C-terminal region, which is related to growth inhibition by up-regulation of $p21^{WAF1}$. HBx protein activates JNK, promoting the oncogenic pSmad3L signaling, which fosters cell growth by up-regulating c-Myc, in a mean time reducing tumor-suppressive pSmad3C-mediated signaling.

The general biomedical approach to HCC is shifting away from population risk assessment and empirical treatment of patients to predictive personalized medicine based on molecular classification and targeted therapy.[29] Better knowledge of the risk factors associated with the occurrence of HCC can improve the effectiveness of surveillance programs. Our approach has identified pSmad3L and pSmad3C as prognostic markers that may prove to be clinically useful. Such predictive markers could allow us to select patients with chronic hepatitis B who have a high or low risk of developing HCC. Although the latter group could be followed up on an annual basis, the patients with a high risk require targeted surveillance measures to allow early diagnosis of HCC.

Phosphorylation of many transcription factors is controlled by the dynamic interplay between kinases and phosphatases. In this regard, we studied the kinetics of both linker and C-terminal phosphorylation of Smad3 in parental and HBx-expressing hepatocytes in response to TGF-β (unpublished observation). In parental hepatocytes, the levels of linker and C-terminal phosphorylation peaked at 30 minutes after the start of exposure to TGF-β and then gradually declined. However, HBx-expressing hepatocytes showed constitutive phosphorylation at Smad3L during continuous exposure to TGF-β. Several lines of evidence have identified small C-terminal domain phosphatase (SCP1-3) and protein phosphatase magnesium 1A (PPM1A) as the linker and C-terminal phosphatases, respectively.[37,38] Accordingly, SCP1-3 and PPM1A may reverse domain-specific phosphorylation in normal hepatocyes. In contrast, HBx-expressing hepatocytes may not show induction or activation of SCP1-3. Alternatively, linker phosphorylation in HBx-expressing hepatocytes might be resistant to SCP1-3.

Many researchers have been seeking key transcription factors regulating tumor-suppressive pathways that are altered in cancer. Our current model of JNK/pSmad3L signaling during HBV-related chronic liver disease suggests that specific inhibitors of the JNK/pSmad3L pathway might inhibit the progression of HCC. With respect to molecular targeting therapy for human HCC, pSmad3L and pSmad3C should be assessed as biomarkers to evaluate the benefit from specific inhibition of the JNK/pSmad3L pathway.

Acknowledgment: We thank Dr. Rik Derynck (University of California at San Francisco) and Dr. Seishi Murakami (Kanazawa University) for providing us with complementary DNAs encoding human Smad3 and HBx. We also thank Chiaki Kitano for assistance to construct ecotropic retrovirus and Natsuko Ohira for assistance with immunoblotting.

Table 5. Variables with Independent Predictive Value for HCC in Univariate and Multivariate Analyses

Characteristics	n	No. of Patients with HCC (%)	Univariate Analysis		Multivariate Analysis	
			Hazard Ratio (95% CI)	P Value	Hazard Ratio (95% CI)	P Value
pSmad3L positivity*						
Low (1 and 2)	32	1 (3)	1.00		1.00	
High (3 and 4)	28	6 (21)	3.8 (1.4-10.6)	0.01	14.8 (1.8-118.5)	0.01
pSmad3C positivity*						
High (3 and 4)	30	0 (0)	1.00		1.00	
Low (1 and 2)	30	7 (23)	2.8 (0.001-7.0)	0.03	16.4 (1.0-125.0)	0.04
Fibrotic stage†						
Low (F1 and F2)	39	4 (10)	1.00		1.00	
High (F3)	21	3 (14)	1.9 (0.7-5.4)	0.24	3.9 (0.4-38.6)	0.24
Inflammatory activity†						
Low (A0 and A1)	23	1 (4)	1.00		1.00	
High (A2 and A3)	37	6 (16)	1.8 (0.7-4.8)	0.27	0.2 (0.02-1.1)	0.06
HBV DNA (copies /mL)						
$<10^5$	42	3 (7)	1.00		1.00	
$>10^5$	18	4 (22)	1.9 (1.0-3.5)	0.05	2.5 (0.9-6.9)	0.08
HBeAg						
Negative	42	4 (10)	1.00		1.00	
Positive	18	3 (17)	2.1 (0.5-9.5)	0.32	9.9 (1.1-89.3)	0.03

Abbreviations: CI, confidence interval; HBeAg, hepatitis B e antigen; HBV, hepatitis B virus; HCC, hepatocellular carcinoma; pSmad3C, C-terminally phosphorylated Smad3; pSmad3L, linker-phosphorylated Smad3.

*Hepatocytic Smad3 phosphorylation in chronic hepatitis B specimens is scored as follows: 0, no phosphorylation; 1, <25% Smad3 phosphorylation; 2, 25% to 50% Smad3 phosphorylation; 3, 50% to 75% Smad3 phosphorylation; 4, >75% Smad3 phosphorylation.

†Necroinflammatory activity and fibrotic stage are determined histologically according to Desmet's classification.

References

1. Llovet JM, Burroughs A, Bruix J. Hepatocellular carcinoma. Lancet 2003; 362:1907-1917.
2. El-Serag HB. Hepatocellular carcinoma: recent trends in the United States. Gastroenterology 2004;127(Suppl):27S–34S.
3. Brechot C, Pourcel C, Louise A, Rain B, Tiollais P. Presence of integrated hepatitis B virus DNA sequences in cellular DNA of human hepatocellular carcinoma. Nature 1980;286:533-535.
4. Kim CM, Koike K, Saito I, Miyamura T, Jay G. HBx gene of hepatitis B virus induces liver cancer in transgenic mice. Nature 1991;351:317-320.
5. Yu DY, Moon HB, Son JK, Jeong S, Yu SL, Yoon H, et al. Incidence of hepatocellular carcinoma in transgenic mice expressing the hepatitis B virus X-protein. J Hepatol 1999;31:123-132.
6. Koike K, Moriya K, Iino S, Yotsuyanagi H, Endo Y, Miyamura T, et al. High-level expression of hepatitis B virus HBx gene and hepatocarcinogenesis in transgenic mice. HEPATOLOGY 1994;19:810-819.
7. Benn J, Su F, Doria M, Schneider RJ. Heptitis B virus HBx protein induces transcription factor AP-1 by activation of extracellular signal-related and c-Jun N-terminal mitogen-activated protein kinases. J Virol 1996;70: 4978-4985.
8. Roberts AB, Sporn MB. The transforming growth factor-βs. In: Sporn MB, Roberts AB, eds. Peptide Growth Factors and Their Receptors. Berlin: Springer-Verlag, 1990:419-472.
9. Heldin CH, Miyazono K, ten Dijke P. TGF-β signaling from cell membrane to nucleus through SMAD proteins. Nature 1997;390:465-471.
10. Massagué J. TGF-β signal transduction. Annu Rev Biochem 1998;67: 753-791.
11. Kretzschmar M, Doody J, Timokhina I, Massague J. A mechanism of repression of TGF-β/Smad signaling by oncogenic Ras. Genes Dev 1999; 13:804-816.
12. Mori S, Matsuzaki K, Yoshida K, Furukawa F, Tahashi Y, Yamagata H, et al. TGF-β and HGF transmit the signals through JNK-dependent Smad2/3 phosphorylation at the linker regions. Oncogene 2004;23:7416-7429.
13. Furukawa F, Matsuzaki K, Mori S, Tahashi Y, Yoshida K, Sugano Y, et al. p38 MAPK mediates fibrogenic signal through Smad3 phosphorylation in rat myofibroblasts. HEPATOLOGY 2003;38:879-889.
14. Matsuura I, Denissova NG, Wang G, He D, Long J, Liu F. Cyclin-dependent kinases regulate the antiproliferative function of Smads. Nature 2004;430:226-231.
15. Yamagata H, Matsuzaki K, Mori S, Yoshida K, Tahashi Y, Furukawa F, et al. Acceleration of Smad2 and Smad3 phosphorylation via c-Jun NH(2)-terminal kinase during human colorectal carcinogenesis. Cancer Res 2005; 65:157-165.
16. Sekimoto G, Matsuzaki K, Yoshida K, Mori S, Murata M, Seki T, et al. Reversible Smad-dependent signaling between tumor suppression and oncogenesis. Cancer Res 2007;67:5090-5096.
17. Arany PR, Rane SG, Roberts AB. Smad3 deficiency inhibits v-ras-induced transformation by suppression of JNK MAPK signaling and increased farnesyl transferase inhibition. Oncogene 2008;27:2507-2512.
18. Yoshida K, Matsuzaki K, Mori S, Tahashi Y, Yamagata H, Furulawa F, et al. Transforming growth factor-β and platelet-derived growth factor signal via c-Jun N-terminal kinase-dependent Smad2/3 phosphorylation in rat hepatic stellate cells after acute liver injury. Am J Pathol 2005;166:1029-1039.
19. Block TM, Mehta AS, Fimmel CJ, Jordan R. Molecular viral oncology of hepatocellular carcinoma. Oncogene 2003;22:5093-5107.
20. Matsuzaki K, Murata M, Yoshida K, Sekimoto G, Uemura Y, Sakaida N, et al. Chronic inflammation associated with hepatitis C viral infection perturbs hepatic TGF-β signaling, promoting cirrhosis and hepatocellular carcinoma. HEPATOLOGY 2007;46:48-57.
21. Desmet VJ, Gerber M, Hoofnagle JH, Manns M, Scheuer PJ. Classification of chronic hepatitis: diagnosis, grading and staging. HEPATOLOGY 1994;19:1513-1520.
22. Cox DR. Regression models and life-tables. J R Stat Soc (B) 1972;34:187-220.
23. Pardali K, Moustakas A. Actions of TGF-β as tumor suppressor and pro-metastatic factor in human cancer. Biochim Biophys Acta 2007;1775:21-62.

24. Chen CJ, Yang HI, Su J, Jen CL, You SL, Lu SN, et al. REVEAL-HBV study group. Risk of hepatocellular carcinoma across a biological gradient of serum hepatitis B virus DNA level. JAMA 2006;295:65-73.
25. Feitelson MA. c-Myc overexpression in hepatocarcinogenesis. Human Pathology 2004;35:1299-1302.
26. Yang HI, Lu SN, Liaw YF, You SL, Sun CA, Wang LY, et al. Taiwan community-based cancer screening project group. Hepatitis B e antigen and the risk of hepatocellular carcinoma. N Engl J Med 2002;347:168-174.
27. Thorgeirsson SS, Lee JS, Grisham JW. Functional genomics of hepatocellular carcinoma. HEPATOLOGY 2006;43:145-150.
28. Theise ND, Park YN, Kojiro M. Dysplastic nodules and hepatocarcinogenesis. Clin Liver Dis 2002;6:497-512.
29. Thorgeirsson SS, Grisham JW. Molecular pathogenesis of human hepatocellular carcinoma. Nat Genet 2002;31:339-346.
30. Chisari FV, Klopchin K, Moriyama T, Pasquinelli C, Dunsford HA, Sell S, et al. Molecular pathogenesis of hepatocellular carcinoma in hepatitis B virus transgenic mice. Cell 1989;59:1145-1156.
31. Moriya K, Fujie H, Shintani Y, Yotsuyanagi H, Tsutsumi T, Ishibashi K, et al. The core protein of hepatitis C virus induces hepatocellular carcinoma in transgenic mice. Nat Med 1998;4:1065-1067.
32. Di Bisceglie AM. Hepatitis C and hepatocellular carcinoma. HEPATOLOGY 1997;26 (Suppl):34S–38S.
33. Popper H, Shafritz DA, Hoofnagle JH. Relation of the hepatitis B virus carrier state to hepatocellular carcinoma. HEPATOLOGY 1987;7:764-772.
34. Inagaki Y, Okazaki I. Emerging insights into transforming growth factor β Smad signal in hepatic fibrogenesis. Gut 2007;56:284-292.
35. Kaimori A, Potter J, Kaimori JY, Wang C, Mezey E, Koteish A. Transforming growth factor-β1 induces an epithelial-to-mesenchymal transition state in mouse hepatocytes in vitro. J Biol Chem 2007;282:22089-22101.
36. Weng HL, Ciuclan L, Liu Y, Hamzavi J, Godoy P, Gaitantzi H, et al. Profibrogenic transforming growth factor-β/activin receptor-like kinase 5 signaling via connective tissue growth factor expression in hepatocytes. HEPATOLOGY 2007;46:1257-1270.
37. Lin X, Duan X, Liang YY, Su Y, Wrighton KH, Long J, et al. PPM1A functions as a Smad phosphatase to terminate TGFβ signaling. Cell 2006; 125:915-928.
38. Wrighton KH, Willis D, Long J, Liu F, Lin X, Feng XH. Small C-terminal domain phosphatases dephosphorylate the regulatory linker regions of Smad2 and Smad3 to enhance transforming growth factor-β signaling. J Biol Chem 2006;281:38365-38375.

THE JOURNAL OF BIOLOGICAL CHEMISTRY VOL. 284, NO. 6, pp. 3513–3520, February 6, 2009

A Single Amino Acid of Toll-like Receptor 4 That Is Pivotal for Its Signal Transduction and Subcellular Localization*

Received for publication, April 22, 2008, and in revised form, October 29, 2008 Published, JBC Papers in Press, December 8, 2008, DOI 10.1074/jbc.M803086200

Shintaro Yanagimoto[‡§¶], Keita Tatsuno[§], Shu Okugawa[§], Takatoshi Kitazawa[§], Kunihisa Tsukada[§], Kazuhiko Koike[§], Tatsuhiko Kodama[¶], Satoshi Kimura[‖], Yoshikazu Shibasaki[‡1], and Yasuo Ota[1,2]**

From the [‡]Center for Structuring Life Sciences, Graduate school of Arts and Sciences, University of Tokyo, Meguro-ku, Tokyo 153-8903, the [§]Department of Infectious Diseases, Graduate School of Medicine, University of Tokyo, Bunkyo-ku, Tokyo 113-8655, the [¶]Laboratory for Systems Biology and Medicine, Research Center for Advanced Science and Technology, University of Tokyo, Meguro-ku, Tokyo 153-8904, the [‖]Tokyo Teishin Hospital, Fujimi, Chiyoda-ku, Tokyo 102-8798, and the [**]Department of Medicine, Teikyo University School of Medicine, 2-11-1, Kaga, Itabashi-ku, Tokyo 173-8605, Japan

Toll-like receptor 4 (TLR4) is essential for recognizing a Gram-negative bacterial component, lipopolysaccharide (LPS). A single amino acid mutation at position 712 of murine TLR4 leads to hyporesponsiveness to LPS. In this study we determined that an amino acid, a leucine at position 815 of human TLR4, is also pivotal for LPS responsiveness and subcellular distribution. By replacing the leucine with alanine, the mutant TLR4 lost responsiveness to LPS and did not localize on the plasma membrane. In addition, it does not coprecipitate with myeloid differentiation-2, an accessory protein that is necessary for TLR4 to recognize LPS. These results suggest that the leucine at position 815 is required for the normal maturation of TLR4 and for formation of the TLR4·MD-2 complex.

Toll-like receptors (TLRs)[3] play essential roles in both innate and adaptive immunity (1). Thirteen members of the TLR family have been identified in mammals. TLRs have leucine-rich-repeats in their extracellular domains and a Toll/Interleukin-1 receptor (TIR) in their cytoplasmic domains, the latter of which mainly mediates intracellular signaling. Signaling pathways of TLRs, except for TLR3, depend on an adapter protein, MyD88 (myeloid differentiation factor 88), which interacts with the TIR domain of TLRs. This pathway leads to the activation of the transcription factor NF-κB and production of cytokines such as tumor necrosis factor-α and interleukin-6. Another important signaling pathway mediated by TLR3 and TLR4 that exploits the TIR domain is the MyD88-independent pathway. This pathway involves different adapter proteins, such as the TIR domain-containing adaptor inducing interferon-β (TRIF) and TRIF-related adaptor molecule (2–4), and is essential for production of type I interferon through activation of interferon regulatory factor-3.

TLRs recognize as ligands several microbial pathogen-associated molecular patterns. One such pathogen-associated molecular pattern is lipopolysaccharide (LPS), which is recognized by TLR4. LPS triggers severe immunologic reactions by the host in Gram-negative bacterial infections and has drawn attention in many clinical situations. TLR4 is the first mammalian TLR to be discovered in the context of immunology. TLR4 was identified in the search for the genes responsible for LPS hyporesponsiveness (5, 6). The defect was found to stem from a single amino acid mutation, replacement of proline with histidine at position 712, in the cytoplasmic tail of murine TLR4. The study led to the discovery of the importance of TLR4 in innate immunity.

A variety of cells are activated by LPS stimulation through TLR4. TLR4 forms a receptor complex with an accessory protein, myeloid differentiation-2 (MD-2). MD-2 first associates with TLR4 in the endoplasmic reticulum (ER) and *cis*-Golgi, and both proteins move together to the plasma membrane (7, 8). Upon recognition of LPS, the TLR4·MD-2 complex receives LPS on the cell surface and initiates intracellular signaling. The expression of TLR4 in the absence of MD-2 does not confer full responsiveness to LPS stimuli in experimental cell lines (9). An analysis of MD-2 knockout mice revealed that MD-2 is important not only for LPS sensing but also for cellular distribution of TLR4.

In this study we hypothesized that the cytoplasmic tail of TLR4 contains regions that control both localization and signaling. Using truncation and mutation analysis, and paying particular attention to the TIR domain, we identified a single amino acid that is pivotal for both TLR4 signaling and subcellular distribution. The site we found was on the C-terminal portion of the TIR domain for which no specific function has been yet determined.

* This work was partly supported by the Program of Fundamental Studies in Health Sciences of the National Institute of Biomedical Innovation, by the Focus 21 project of the New Energy and Industrial Technology Development Organization, and by the Special Coordination Fund for Science and Technology from the Ministry of Education, Culture, Sports, Science and Technology. This study was also partly supported by a grant-in-aid from the Ministry of Education, Culture, Sports, Science and Technology (to Y. O.). The costs of publication of this article were defrayed in part by the payment of page charges. This article must therefore be hereby marked "*advertisement*" in accordance with 18 U.S.C. Section 1734 solely to indicate this fact.

[1] Both authors contributed equally to this work.

[2] To whom correspondence should be addressed. Tel.: 81-3-3964-1211 (ext. 1756); Fax: 81-3-3579-6310; E-mail: yasuota-tky@umin.ac.jp.

[3] The abbreviations used are: TLR, Toll-like receptor; TIR, Toll/Interleukin-1 receptor; TRIF, TIR domain-containing adaptor inducing interferon-β; LPS, lipopolysaccharide; MD-2, myeloid differentiation-2; ER, endoplasmic reticulum; GFP, green fluorescent protein; EGFP, enhanced GFP; RLA, relative luciferase activity; Sulfo-NHS-SS-Biotin, sulfosuccinimidyl-2-(biotinamido)ethyl-1,3-dithiopropionate.

EXPERIMENTAL PROCEDURES

Reagents and Other Materials—Lipopolysaccharide (LPS) from *Escherichia coli* O55:B5 was purchased from Sigma-Aldrich and applied without repurification. FLAG- and hexa-histidine (His_6)-tagged human TLR4 expression plasmid (pEFBOS/humanTLR4flaghis) and FLAG- and His_6-tagged human MD-2 expression plasmid (pEFBOS/humanMD-2flaghis) were generous gifts from Dr. Kensuke Miyake (Institute of Medical Science, University of Tokyo, Japan). Human CD14 cDNA plasmid (pCMV6-XL5/humanCD14) was purchased from OriGene (Rockville, MD). Fluorescent protein expression vector pEGFP-N3 was purchased from Clontech (Mountain View, CA). Anti-TLR4 monoclonal antibody (clone HTA125) was purchased from Abcam (Cambridge, MA). Anti-FLAG monoclonal antibody (clone M2) was purchased from Sigma-Aldrich. Anti-*A.v.* (GFP) monoclonal and polyclonal antibodies were purchased from Clontech. Control immunoglobulins for immunoprecipitation were purchased from BD Biosciences (San Jose, CA). Horseradish peroxidase-labeled anti-immunoglobulins antibodies were purchased from Dako (Glostrup, Denmark). BlockAce (DS Pharma Biomedical, Osaka, Japan) solution was used as blocking buffer for Western blotting.

Cell Culture—Human embryonic kidney (HEK) 293T cells were maintained in Dulbecco's modified Eagle's medium (Sigma-Aldrich) containing 10% heat-inactivated fetal bovine serum supplemented with penicillin-streptomycin solution (Invitrogen). FuGENE 6 transfection reagent (Roche Applied Science) was used for transient cotransfection according to the manufacturer's instructions. Culture dishes or plates were prepared to 70% confluence prior to transfection. Cells were used for experiments 36 h later. The transfection conditions were optimized for microscopic observation of the expressed fluorescent protein and were kept unchanged in other experiments.

Expression Vector Subcloning and Mutagenesis—Wild-type TLR4 cDNA was excised from pEFBOS/humanTLR4flaghis and subcloned into pEGFP-N3 so that when expressed enhanced green fluorescent protein (EGFP) would be fused at the C terminus of TLR4 (pEGFP-N3/humanTLR4). All mutations were introduced into pEFBOS/humanTLR4flaghis and pEGFP-N3/humanTLR4 using the QuikChange site-Directed mutagenesis kit (Stratagene, La Jolla, CA) according to the manufacturer's instructions and were confirmed by sequencing. For the truncation analysis, two identical unique restriction sites were prepared in the TLR4-coding region of pEFBOS/humanTLR4 using a QuikChange kit, and the DNA fragment to be removed, which was a part of the C terminus of TLR4, was excised enzymatically. After agarose gel purification, the linear double-stranded DNA was ligated to re-form a circular plasmid. Restriction sites were designed so as not to cause a frameshift between TLR4 and EGFP.

Confocal Laser Scanning Microscopy of Cells—Samples were fixed in 3% paraformaldehyde-phosphate-buffered saline at 37 °C for 10 min. Fluorescence images of fixed samples were recorded using a FluoView FV1000 Confocal Microscope (an inverted confocal laser scanning microscope, Olympus, Tokyo, Japan).

Immunoprecipitation—Transfected cells were lysed in lysis buffer (50 mM Tris-HCl, pH 7.5, 100 mM NaCl, 0.1% Triton X-100, 1 mM 1,4-dithiothreitol, and proteinase inhibitor mixture), sonicated, and centrifuged at 4 °C. Antibody was added to the supernatant, and the sample was rotated 1 h at 4 °C followed by the addition of protein G-Sepharose (GE Healthcare Life Sciences, Piscataway, NJ) and an additional 8-h incubation at 4 °C. Bound protein was washed three times in lysis buffer. Proteins were eluted by boiling in SDS sample buffer.

Biotinylation and Purification of Cell Surface Proteins—Prior to surface biotinylation, HEK 293T cells plated in a 100-mm dish were transiently transfected as described above. Surface biotinylation and subsequent purification of biotinylated proteins were performed using a Cell Surface Protein Biotinylation and Purification Kit (Pierce) following the manufacturer's instructions. Briefly, membrane-impermeable sulfosuccinimidyl-2-(biotinamido)ethyl-1,3-dithiopropionate (Sulfo-NHS-SS-Biotin) was added to cell monolayers in the culture dishes and covalently bound to amines in proteins exposed on the cell surface. The affinity resin that binds to the biotin end of Sulfo-NHS-SS-Biotin was used to collect the biotinylated proteins. Reduction by 1,4-dithiothreitol causes cleavage of the disulfide bond in Sulfo-NHS-SS-Biotin, and the elute contains the biotinylated cell surface proteins. Each final sample obtained was considered to contain proteins from an equal amount of cells, because all culture plates were treated equally and grown to full confluence. All samples were sonicated and subjected to SDS-PAGE and Western blotting. The membrane to which protein was transferred was blocked in blocking buffer for 1 h. Then the membrane was incubated with a primary antibody, followed by incubation with horseradish peroxidase-labeled anti-immunoglobulins antibody. The protein bands were then visualized by using a chemiluminescence reagent, Immobilon Western Chemiluminescent HRP Substrate (Millipore, Billerica, MA), according to the manufacturer's instructions.

Cell Stimulation Assays—HEK293T cells were plated and transiently transfected for assays. Thirty-six hours after the transfection, LPS was added to fresh culture medium in each well of the culture plates at the stated concentration. The duration of LPS stimulation was 7 h.

Dual Luciferase Reporter Assays for NF-κB Activation—HEK293T cells were plated in 12-well culture plates (4×10^4 cells/well), and experimental cDNA plasmids were transiently transfected 36 h later using the FuGENE 6 transfection reagent with 0.5 μg of NF-κB reporter plasmid expressing firefly luciferase (pNF-κB-Luc, Stratagene) and 0.05 μg of constitutively active *Renilla* luciferase reporter plasmid (pRL-TK, Promega, Madison, WI) in addition to 0.5 μg each of TLR4-EGFP plasmid and MD-2 plasmid. Stimulation experiments were performed 36 h later. Firefly luciferase and *Renilla* luciferase activities were measured using the Dual-Luciferase Reporter Assay System (Promega) and the Genelight55 luminometer (Microtech, Chiba, Japan). Relative luciferase activity (RLA) was obtained as the ratio of firefly luciferase activity to *Renilla* luciferase activity. Results are expressed as the ratio of RLA with LPS stimulation to RLA without LPS stimulation ([RLA LPS+]/[RLA LPS−]). This ratio should ideally approach 1 when no response to LPS stimulation is observed.

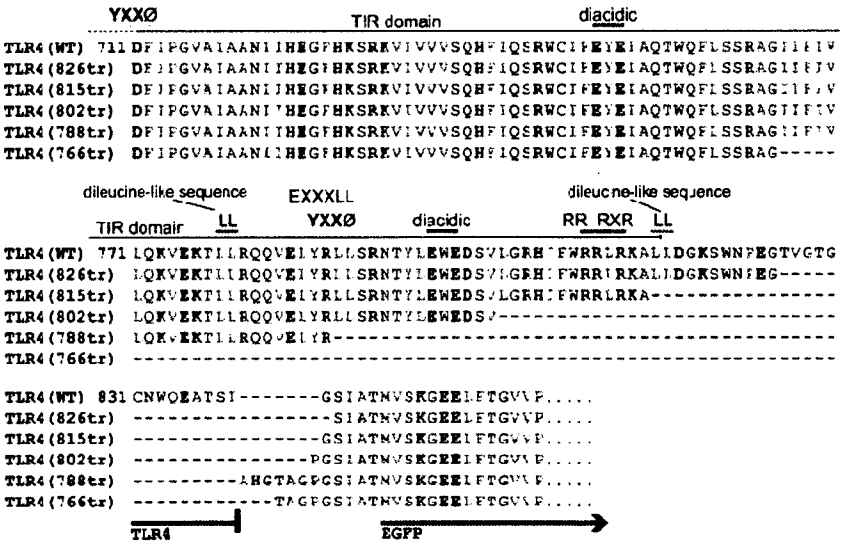

FIGURE 1. **Alignment of the cytoplasmic domains of EGFP fusion TLR4 truncation mutants used in this study.** TLR4 (766tr) signifies the mutant truncated at position 766. Others are named in the same manner. The amino acids are colored based on their physicochemical properties: *pink*, basic; *blue*, acidic; *green*, polar and neutral; and *orange*, hydrophobic. The *black overline* represents the TIR domain. *Colored overlines* indicate amino acid sequences identical to known sorting signal motifs except for two LLs, which are dileucine motif-like sequences in that they consist of solely two consecutive leucines without preceding aspartate or glutamate. *Capital letters* on the *line* signify the single-letter code for amino acids: *E*, glutamic acid; *L*, leucine; *R*, arginine; and *Y*, tyrosine. *X* signifies any amino acid, and *Ø* signifies an amino acid residue with a bulky hydrophobic side chain.

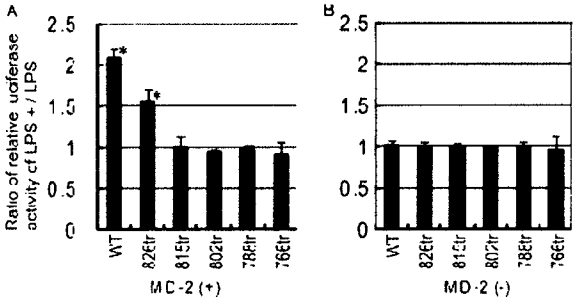

FIGURE 2. **LPS responsiveness measured by NF-κB luciferase assay.** HEK293T cells were transfected with plasmids containing the gene for wild-type TLR4 or a truncated human TLR4-EGFP fusion protein, in addition to a luciferase reporter and human MD-2 plasmid (*A*) or unmodified plasmids (control) (*B*). After 36 h, cells were stimulated with LPS (10 ng/ml) for 7 h, and luciferase reporter gene activity was measured. All results were expressed as the ratio of relative luciferase activity with LPS stimulation to that without stimulation. The data were from three independent experiments. *Small bars* indicate 95% confidence intervals of the mean (p values for * are: TLR4 (WT)-EGFP/MD-2 (+), $p = 0.002$; TLR4 (826tr)-EGFP/MD-2 (+), $p = 0.016$).

Statistical Analyses—All quantitative experiments were repeated three times, and each experiment was done in triplicate. The ratio of relative luciferase activity of LPS+ to LPS− was calculated as the index of the responsiveness to the stimuli as explained above. When positive response is observed, the ratio should significantly exceed one. The means of the ratio were represented in *bar graphs*. The 95% confidence interval of the mean of the ratio was calculated and indicated on each *bar* in the *graph*, and p values were calculated using Student's t distribution compared with the hypothetical mean, one.

RESULTS

Truncation Analysis of TLR 4—To identify amino acid sequences in the cytoplasmic tail of TLR4 that are involved in both signal transduction and subcellular distribution, first we generated five truncation mutants of TLR4 with a fluorescent protein (EGFP) at the C terminus of TLR4.

Although there are no known definite sorting signal motifs in the cytoplasmic tail of TLR4, some amino acid sequences are similar or identical to known general sorting signal motifs as shown in Fig. 1. *YXXØ*, a form of tyrosine-based sorting signal, and *EXXXLL*, a form of dileucine (LL)-based sorting signal, both control protein internalization, lysosomal targeting, and basolateral targeting (10), where "*X*" represents any amino acid, "*Ø*" stands for an amino acid residue with a bulky hydrophobic side chain, and other letters are single-letter abbreviations for the amino acids. "Diacidic" signals such as D*X*E mediate export from the ER (11). RR or R*X*R is another example of an ER export signal (12). Truncation sites were chosen so that some of these amino acid sequences were deleted in each mutant. Because the TIR domain, which is essential in TLR4 signaling and possibly subcellular localization (13), spans most of the cytoplasmic domain of TLR4, four out of five mutants have involvement in the TIR domain, which we hypothesized could result in impaired signal transduction and a change in subcellular distribution. Part of the cytoplasmic portion of the amino acid sequence of the truncation mutants is shown in Fig. 1. The five truncation mutant proteins lost their C-terminal tails at positions 826, 815, 802, 788, and 766, respectively, and were conjugated with EGFP *in vitro*. Actual truncation and ligation sites of all actual mutants were confirmed to have the designed DNA alignment by sequencing.

We utilized the luciferase reporter assay to assess NF-κB transcription activity as an indicator of TLR4 response to LPS stimuli. MD-2 is reported to be essential for this response (9). However, because it is not known whether MD-2 is necessary for transduction of the truncated TLR4 signal as well, we performed the assays with and without MD-2. The index of cell responsiveness to the stimulation was measured as the ratio between RLA with LPS stimulation and RLA without LPS stimulation. Only cells transfected with TLR4 (826tr)-EGFP in combination with MD-2 retained responsiveness to LPS stimulation. One exception was wild-type TLR4-EGFP (Fig. 2*A*). HEK293T cells transfected with TLR4 but without MD-2 did not respond to LPS stimuli regardless of the TLR4-EGFP genotype (Fig. 2*B*).

Next, we compared the localization of wild-type and truncated mutants of TLR4-EGFP in HEK293T by fluorescence microscopy (Fig. 3*A*). The wild-type TLR4 cotransfected with MD-2 was expressed on the plasma membrane and also in the

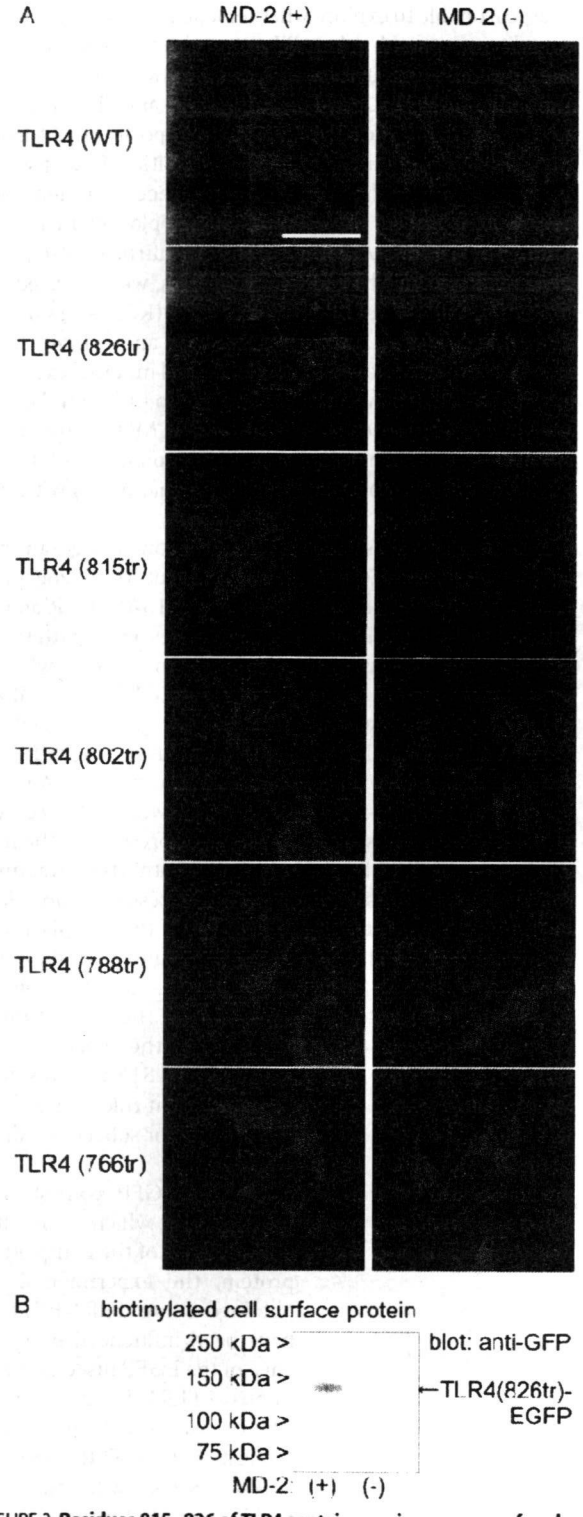

FIGURE 3. **Residues 815–826 of TLR4 contain a region necessary for plasma membrane localization.** *A*, cells were cultured on coverslips in 12-well plates and transfected as in Fig. 2. EGFP-tagged TLR4 was visualized by laser confocal microscopy. Fluorescence from EGFP was observed in *green*. Each genotype of TLR4-EGFP was cotransfected with a human MD-2 plasmid or empty vector. *Bar*, 20 μm. *B*, TLR4 (826tr)-EGFP with or without coexpression of MD-2 were tagged by biotinylation of the cell surface proteins and affinity-purified. TLR4 was visualized by immunoblotting using an anti-GFP monoclonal antibody. Samples from both combinations of DNAs were prepared from the same number of cells.

perinuclear area. These findings were consistent with observations by others (14, 15). TLR4 is reported to localize in the Golgi apparatus as well as on the plasma membrane. Our observation of TLR4-EGFP accumulation in the perinuclear area does not contradict the report that TLR4 partly localizes in the Golgi apparatus (14).

TLR4-EGFP truncation mutants, 815tr, 802tr, 788tr, and 766tr apparently did not localize at the plasma membrane. No particular fluorescence pattern that might be characteristic of localization to a specific intracellular compartment was observed. Only TLR4 (826tr)-EGFP, which has the shortest truncation, was expressed on the plasma membrane and in the perinuclear area, and the fluorescence pattern was similar to that of wild-type (Fig. 3*A*). No TLR4 genotypes, including wild-type TLR4-EGFP, clearly localized on the plasma membrane in the absence of MD-2 (Fig. 3*A*). MD-2 is reported to be necessary for localization of wild-type TLR4 at the plasma membrane (15), which is consistent with our observation. Intracellular distribution of mutant TLR4 varied depending on the genotype, but no particular cellular structure was identified as an alternative target site. Furthermore, we examined the plasma membrane expression of TLR4 (826tr)-EGFP by cell surface protein biotinylation. The expression level of TLR4 (826tr)-EGFP was markedly decreased without coexpression of MD-2 (Fig. 3*B*), which is compatible with the microscope observation.

Removal of the C-terminal segment of TLR4 at residue 826 does not qualitatively affect LPS responsiveness and subcellular distribution. However, when more residues, up to position 815, were removed, both signal transduction and plasma membrane localization were impaired. These results suggest that residues 815–826 of TLR4 contain at least one segment that is critical for those functions.

Amino Acid Sequence Replacement Analysis—To identify critical amino acid sequences in this region, we generated an amino acid replacement mutant of TLR4 instead of truncation mutants. As shown in Fig. 1, although it is not a canonical sequence, leucine-leucine at 815–816 partially fits a known sorting signal motif, a dileucine motif, (D/E)*XXX*L(L/I) or D*XX*LL, which plays an important role in internalization of plasma membrane protein or sorting from the *trans*-Golgi network (10). Thus, as has been done in a similar study (16), a mutant was generated in which alanines were substituted for both leucines at positions 815 and 816.

We measured the NF-κB activity of TLR4 (L815AL816A)-EGFP, the mutant in which both leucines were replaced with alanines, under LPS stimulation (Fig. 4*A*). This mutant protein did not respond to LPS stimuli. Microscopic observation revealed that TLR4 (L815AL816A)-EGFP was not expressed on the plasma membrane regardless of whether MD-2 was cotransfected (Fig. 4*B*). The phenotype of this doubly substituted mutant appeared to be the same as that of the truncation mutants. These results imply that the leucines in positions 815 and 816 play an important role in TLR4 plasma membrane localization.

Analysis of Single Amino Acid Substitution Mutants—As previously mentioned, the amino acid sequence leucine-leucine at positions 815 and 816 does not completely match the dileucine motif, *i.e.* it lacks a preceding acidic amino acid. Therefore it

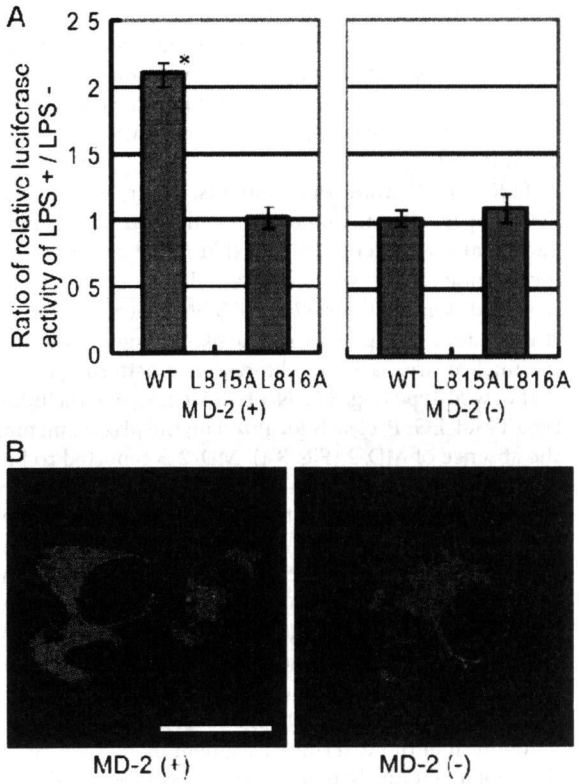

FIGURE 4. **Leucines at positions 815–816 of TLR4 are responsible for impairment of LPS responsiveness and plasma membrane expression.** *A*, the LPS stimulation assay was done for TLR4 (L815AL816A)-EGFP as in Fig. 2. The data were from three independent experiments. *Small bars* indicate 95% confidence intervals of the mean (*p* value for * are: TLR4 (WT)-EGFP/MD-2 (+), $p = 0.002$). *B*, TLR4 (L815AL816A)-EGFP expression in HEK293T cells was observed by laser confocal microscopy. *Bar*, 20 μm.

was reasonable to explore whether leucines 815 and 816 need to be adjacent to each other. We created five genotypes of single amino acid mutants of TLR4: TLR4 (K813A)-EGFP, TLR4 (L815A)-EGFP, TLR4 (L816A)-EGFP, and TLR4 (D817A)-EGFP. We excluded the amino acid at position 814 from the analysis, because the amino acid in position 814 of wild-type TLR4 is alanine. The amino acid sequence alignment of wild-type TLR4 and the single amino acid replacement mutants is shown in Fig. 5. DNA sequences were confirmed by sequencing.

As was done with truncation mutants, we measured NF-κB activity of wild-type TLR4-EGFP, TLR4 (K813A)-EGFP, TLR4 (L815A)-EGFP, TLR4 (L816A)-EGFP, and TLR4 (D817A)-EGFP in response to LPS stimulation. All mutants except TLR4 (L815A)-EGFP showed responsiveness to LPS stimulation with coexpression of MD-2 (Fig. 6*A*). Without MD-2, no genotype of TLR4-EGFP responded to LPS stimulation (Fig. 6*B*). LPS stimulation was performed in an identical manner as with truncation mutants.

We analyzed the subcellular distribution of single amino acid mutants of TLR4-EGFP with and without MD-2 coexpression by fluorescence microscopy. TLR4 (K813A)-EGFP and TLR4 (D817A)-EGFP showed a similar fluorescence pattern to the wild-type, which localized at the plasma membrane when coexpressed with MD-2. No genotypes of TLR4-EGFP localized on the plasma membrane without MD-2 (Fig. 7). The cells transfected with TLR4 (L815A)-EGFP coexpressed with MD-2 did not show plasma membrane fluorescent pattern. Also, TLR4 (L815A)-EGFP showed comparatively weaker fluoresce than other mutants, possibly due to lower expression of the protein. Fluorescence of TLR4 (L816A)-EGFP with MD-2 was ambiguous as for the plasma membrane expression. Some kind of membranous structure was observed in the cytoplasmic area, but the intensity of the plasma membrane green fluorescence was obscure. Together with the results from the LPS stimulation experiment, the leucines at positions 815 and 816 are considered to play important roles in signal transduction and/or subcellular distribution of TLR4.

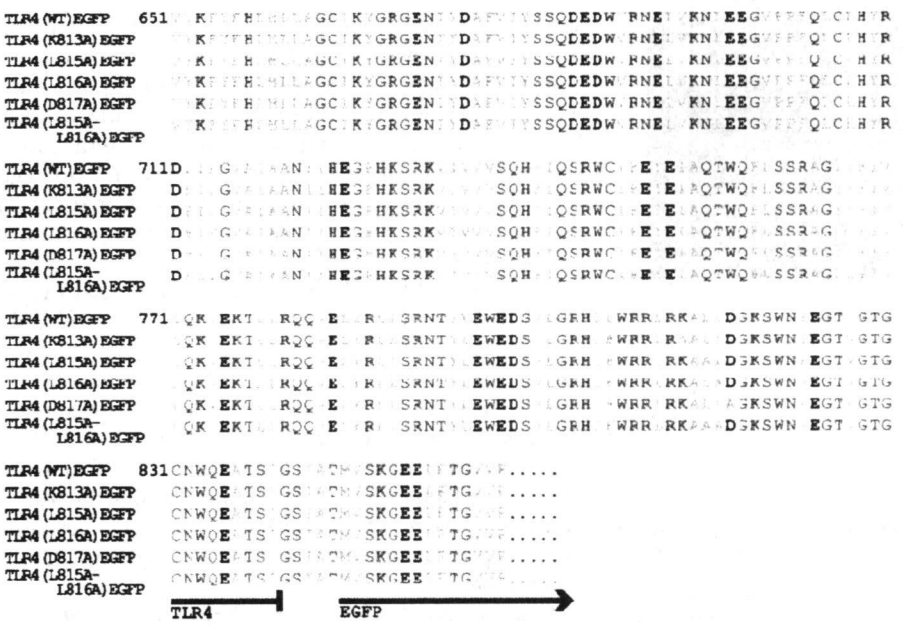

FIGURE 5. **Alignment of the cytoplasmic domain of EGFP fusion TLR4 amino acid-replacement mutants used in this study.** TLR4 (L813A) signifies a mutant with leucine replaced with alanine at position 813. Others are named in the same manner. The amino acids are *colored* as in Fig. 1. All amino acids are designated using the single-letter code.

Because EGFP consists of 239 amino acids, which is about one-third the size of the complete TLR4 protein, the experimental results obtained using TLR4-EGFP could have been influenced by the presence of the EGFP fused at the C terminus of TLR4. To rule out this possibility, we tested the functional integrity of both TLR4 (L815A) and TLR4 (L816A) with and without EGFP at the C terminus. Reporter assays were performed under the same conditions except that the shorter tag, FLAG-His_6, which has only 21-amino acid tags at the C terminus, was fused to TLR4 in place of EGFP. There was no difference

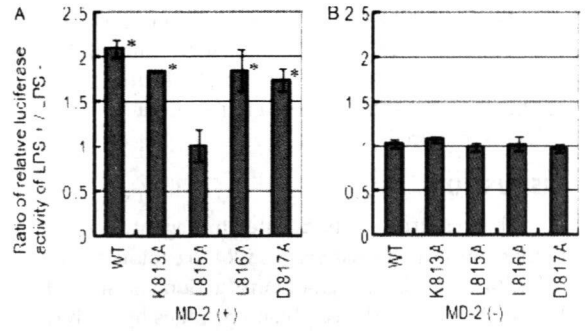

FIGURE 6. **Leucine at position 815 of TLR4 is pivotal for LPS responsiveness as measured by NF-κB luciferase assay.** *A*, HEK293T cells were transfected with single amino acid replacement mutants of the human TLR4-EGFP fusion protein plasmid, human MD-2 plasmid, and luciferase reporter and control plasmids. After 36 h, cells were stimulated with LPS (10 ng/ml) for 7 h, and luciferase reporter gene activity was measured. *B*, instead of MD-2, an empty vector was cotransfected with TLR4-EGFP plasmid and reporter assay vectors. LPS stimulation was done as in *A*. All results were expressed in the ratio of relative luciferase activity with LPS stimulation to that without the stimulation as in Fig. 2. The data were from three independent experiments. *Small bars* indicate 95% confidence intervals of the mean (p values for * are: TLR4 (WT)-EGFP/MD-2 (+), $p = 0.002$; TLR4 (K813A)-EGFP/MD-2 (+), $p = 0.000$; TLR4 (L816A)-EGFP/MD-2 (+), $p = 0.018$; and TLR4 (D817A)-EGFP/MD-2 (+), $p = 0.007$).

between EGFP-tagged proteins and FLAG-His_6-tagged proteins in the relative pattern of responsiveness against LPS stimulation (Fig. 8*A*). Because CD14 is also important for LPS recognition by TLR4, we examined the effect of CD14 coexpression on the phenotypic changes of the mutants (17, 18). Coexpression of CD14 did not change the phenotypes of wild-type TLR4, TLR4 (L815A), and TLR4 (L816A) in terms of LSP responsiveness (data not shown).

Cell surface expressions of the wild-type, L815A mutant, and L816A mutant TLR4-FLAG- His_6 fusion proteins were also examined. Live cells transfected with wild-type TLR4, the L815A mutant or the L816A mutant as well as human MD-2 and CD14 were biotinylated on the cell surface, and the biotinylated proteins were affinity-purified and subjected to Western blotting. Fig. 8*B* shows the marked difference in cell surface expression of wild-type and mutants L815A and L816A. Note that biotinylated proteins have additional residues on every amine of the extracellular domain, which leads to a band shift during electrophoresis. Although both mutants were detected far less than the wild-type on the cell surface, comparatively more L816A mutant was expressed on the plasma membrane than L815A mutant, and the amount of L815A mutant seemed to be negligible compared with the wild type. These results may clarify the ambiguity of the microscopic observation of TLR4 (L815A) and TLR4 (L816A). Plasma membrane expression of TLR4 was impaired when the leucine at 815 or 816 was replaced to alanine. But the leucine at 815 is more critical, and the mutant L816A may show the weaker phenotypic change.

To further investigate the characteristics of the TLR4 (L815A) mutant, we performed an immunoprecipitation assay of wild-type and mutant TLR4. Cells were transfected with a human MD-2-FLAG-His_6 expression vector and either the wild-type or the mutant (L815A) TLR4-EGFP expression vector. Anti-TLR4 monoclonal antibody (clone HTA125), anti-GFP polyclonal antibody, or anti-FLAG monoclonal antibody

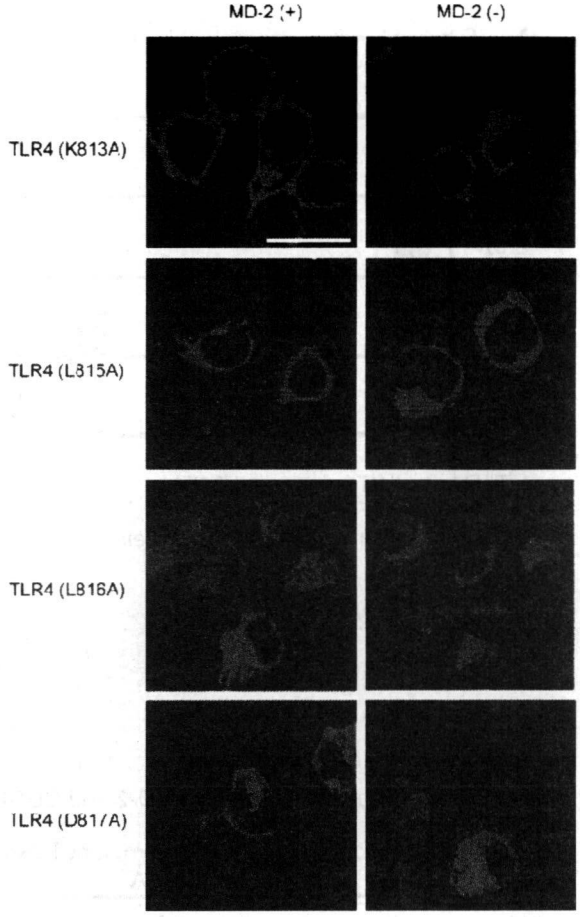

FIGURE 7. **Leucines at the position 815 and 816 of TLR4 are responsible for full plasma membrane expression.** Cells were cultured on coverslips in 12-well plates and transfected as in Fig. 2. EGFP-tagged TLR4 was visualized by laser confocal microscopy. Each genotype of TLR4-EGFP was cotransfected with human MD-2 plasmid or empty vector. *Bar*, 20 μm.

was added to the lysate and precipitated with Protein G-Sepharose beads. Collected proteins were eluted and subjected to Western blotting. The results are shown in Fig. 8*C*. TLR4 (L815A) was not immunoprecipitated with anti-TLR4 antibody (HTA125). HTA125 antibody was raised against TLR4-expressing cells (9) and recognizes the extracellular portion of TLR4. This result suggests that the amino acid replacement at position 815 may cause a change in the extracellular portion of TLR4 and/or that the replacement may also inhibit cell surface expression of the mutant protein. On the other hand, both wild-type TLR4-EGFP and mutant TLR4-EGFP were immunoprecipitated with anti-GFP polyclonal antibody, which recognized EGFP. However, of the two bands of TLR4, the heavier band seems to be somewhat faint in the mutant, whereas in the wild type the heavier band is at least as dense as the lighter one. TLR4 can be detected as two separate bands in a Western blot (19), especially under transient transfection conditions. The difference in proportion of the heavy and light bands between wild-type and mutant TLR4 may suggest that there is some difference in glycosylation. Furthermore, wild-type TLR4 was coprecipitated with MD-2-FLAG-His_6, but the mutant TLR4 could not be detected (Fig. 8*C*, *lanes 4* and *8*). Because MD-2 is

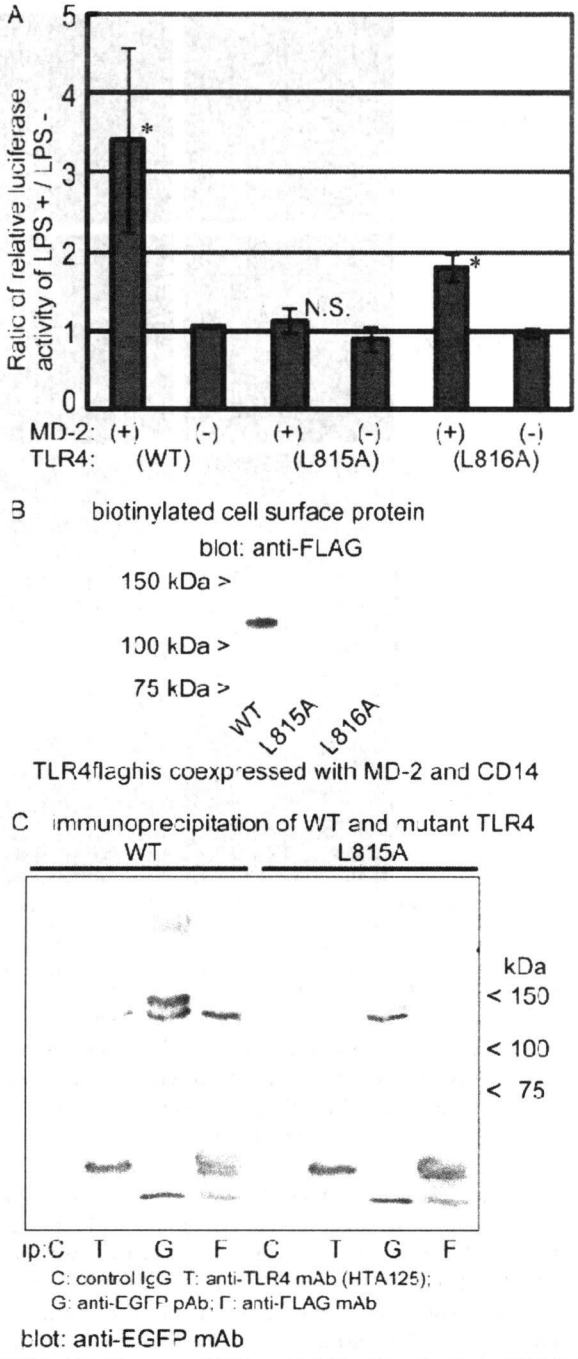

FIGURE 8. *A*, TLR4 mutants L815A and L816A with and without EGFP fusion exhibit the same phenotypes in LPS responsiveness and plasma membrane expression. HEK293T cells were transfected with the wild-type, the L815A or L816A mutant TLR4flaghis plasmid plus the human MD-2 plasmid and luciferase reporter, or control plasmids. After 36 h, cells were stimulated with LPS (10 ng/ml) for 7 h, and luciferase reporter gene activity was measured. The data were from three independent experiments. *Small bars* indicate 95% confidence intervals of the mean (p values for * are: TLR4 (WT) flaghis/MD-2 (+), $p = 0.046$; TLR4 (L816A) flaghis/MD-2 (+), $p = 0.003$). *N.S.*: not significant. *B*, wild-type and mutant TLR4s L815A and L816A were tagged by biotinylation of the cell surface proteins and affinity-purified. Human MD-2 and CD14 were coexpressed. TLR4 was visualized by immunoblotting using an anti-FLAG monoclonal antibody (*mAb*). Faint bands below 100 kDa are considered to be unbiotinylated intracellular TLR4 proteins that were not washed off during the process. Samples from TLR4 (WT), TLR4 (L815A), and TLR4 (L816A), respectively, were prepared from the same number of cells as for the biotinylation experiment. *C*, immunoprecipitation with antibodies further reveals the characteristics of TLR4 (L815A). Anti-TLR4 monoclonal antibody (HTA125) does not precipitate the mutant TLR4, whereas anti-GFP polyclonal antibody (*pAb*) precipitates both wild-type and mutant TLR4. Mutant TLR4 was not coprecipitated with MD-2-FLAG-His_6. Lysates were prepared from cells transiently expressing wild-type or mutant TLR4-EGFP and MD-2-FLAG-His_6.

associated with TLR4 (9), it is logical to expect that immunoprecipitating MD-2-FLAG-His_6 with anti-FLAG antibody should cause TLR4 to be coprecipitated with it. It is suggested by the result here that the association of the TLR4 mutant with MD-2 is impaired.

DISCUSSION

In this research, we performed mutagenesis analyses of particular amino acid residues in TLR4 to explore the mechanisms of TLR4 intracellular signal transduction and subcellular distribution. We found the candidate residues by analyzing truncation mutants of TLR4 in the cytoplasmic region, in which both signaling and normal subcellular distribution of TLR4 are disturbed. Because we are focusing on a common mechanism for the impaired signaling and distribution, we finally picked a single amino acid mutant that does not respond to LPS stimuli, as measured with NF-κB reporter luciferase assay, and one that does not localize on the plasma membrane. TLR4 (L815A) is a mutant that meets these conditions, and our results suggest that the leucine at position 815 of TLR4 is required for both signal transduction and plasma membrane localization.

The best known single amino acid mutant of TLR4 is TLR4 (P712H) known as the *Lps*^{d} mutation in the C3H/HeJ mouse, which corresponds to position 714 in this study of human TLR4 (5, 6, 20). Mice carrying this mutation opened up the rediscovery of TLR4 as a key player in innate immunity. Because this proline residue at this position is within the TIR domain and is conserved among TLRs or TLR4s of other species, it is assumed that the residue plays an important role in TLR4 function. The association of TLR4 (P712H) with its adapter proteins is reported to be intact, and the explanation for the functional impairment of TLR4 (P712H) is not clear (21–23).

Some single amino acid variants are found in humans, and these are related to the incidence or prognosis of some infections and other diseases. A growing body of data suggests that the ability of certain individuals to respond properly to TLR4 ligands may be impaired by single-nucleotide polymorphisms within TLR4 genes (24). The D299G and T399I alleles of the TLR4 gene have been associated with increased risk of severe infections (25).

By clarifying the subcellular component where the mutant protein is retained, or by clarifying to which compartment the mutant is not delivered, the abnormal intracellular sorting that is caused by the mutation in TLR4 (L815A) could be elucidated more precisely. Usually a sorting signal motif is comprised of several amino acids. In this regard, if the leucine at position 815 is a part of a motif, there should be other amino acids that are also members of the motif. Although replacement of leucine with alanine at position 816 did not cause an apparent signal transduction impediment, plasma membrane expression of TLR4 (L816A) was impaired to a certain extent. Positive

response to LPS stimulation by TLR4(L816A) could be attributable to this small amount of expression on the plasma membrane. Mutagenesis analyses of neighboring amino acids of the leucine at 815 were not definitive, but the results could be suggestive that the adjacent leucine at 816 may work together with the leucine at 815. Leucines at position 815 and 816 could be in the same motif, and the leucine at position 816 may be less critical.

Several proteins have been reported to be involved in TLR4 cell surface expression. Heat shock protein gp96 is necessary for TLR4 association with MD-2 in the ER and for subsequent cell surface expression (26). PRAT4A and PRAT4B are associated with TLR4 and regulate TLR4 cell surface expression (27, 28). In embryonic fibroblasts of MD-2 knockout mice, TLR4 localization on the cell surface is severely impaired, and most TLR4 is retained in the ER or Golgi apparatus (15). MD-2 binds to TLR4 at its extracellular domain and is essential for LPS recognition by TLR4 (29). Although proteins such as CD14 and LPS-binding protein are reported to have important roles in LPS recognition by TLR4, in an *in vitro* setting HEK293T cells gain LPS responsiveness by introducing only TLR4 and MD-2 genes when measured by NF-κB reporter assay (9, 30). Without transfection, HEK293 cells do not express TLR4, MD-2, or CD14, which are involved in LPS-induced intracellular signaling (31, 32). In this study, we show that the association of the TLR4 mutant and MD-2 is impaired (Fig. 8*C*).

Post-translational modification is another important factor for TLR4 function. Asparagine residues in the extracellular portion of TLR4 need to be glycosylated for plasma membrane expression of TLR4 (15, 19, 33). TLR4·MD-2 association is necessary for this glycosylation as well. The difference in the proportion of the heavy band to lighter band between wild-type and L815A mutant TLR4 immunoprecipitated with anti-GFP polyclonal antibody suggests that there may be some difference in glycosylation between wild-type and L815A mutant TLR4 (Fig. 8*C*). Although leucine at position 815 is located in the cytoplasmic tail of TLR4, we speculated that substitution of leucine at position 815 may cause a conformational change in the extracellular portion of the protein, which may interfere with the association between L815A mutant TLR4 and MD-2, leading to inhibition of glycosylation and cell surface expression of the mutant protein. Further investigation may reveal the mechanism involved in this phenotypic change in TLR4 (L815A), which would lead to better understanding of the mechanism of wild-type TLR4 signaling and trafficking.

Acknowledgment—We greatly appreciate the gift of human TLR4 and MD-2 cDNA from Dr. Kensuke Miyake (Institute of Medical Science, University of Tokyo, Japan).

REFERENCES

1. Takeda, K., Kaisho, T., and Akira, S. (2003) *Annu. Rev. Immunol.* **21**, 335–376
2. Hoebe, K., Du, X., Georgel, P., Janssen, E., Tabeta, K., Kim, S. O., Goode, J., Lin, P., Mann, N., Mudd, S., Crozat, K., Sovath, S., Han, J., and Beutler, B. (2003) *Nature* **424**, 743–748
3. Oshiumi, H., Sasai, M., Shida, K., Fujita, T., Matsumoto, M., and Seya, T. (2003) *J. Biol. Chem.* **278**, 49751–49762
4. Yamamoto, M., Sato, S., Mori, K., Hoshino, K., Takeuchi, O., Takeda, K., and Akira, S. (2002) *J. Immunol.* **169**, 6668–6672
5. Qureshi, S. T., Lariviere, L., Leveque, G., Clermont, S., Moore, K. J., Gros, P., and Malo, D. (1999) *J. Exp. Med.* **189**, 615–625
6. Poltorak, A., He, X., Smirnova, I., Liu, M. Y., Van Huffel, C., Du, X., Birdwell, D., Alejos, E., Silva, M., Galanos, C., Freudenberg, M., Ricciardi-Castagnoli, P., Layton, B., and Beutler, B. (1998) *Science* **282**, 2085–2088
7. Visintin, A., Mazzoni, A., Spitzer, J. A., and Segal, D. M. (2001) *Proc. Natl. Acad. Sci. U. S. A.* **98**, 12156–12161
8. Nishitani, C., Mitsuzawa, H., Hyakushima, N., Sano, H., Matsushima, N., and Kuroki, Y. (2005) *Biochem. Biophys. Res. Commun.* **328**, 586–590
9. Shimazu, R., Akashi, S., Ogata, H., Nagai, Y., Fukudome, K., Miyake, K., and Kimoto, M. (1999) *J. Exp. Med.* **189**, 1777–1782
10. Bonifacino, J. S., and Traub, L. M. (2003) *Annu. Rev. Biochem.* **72**, 395–447
11. Nishimura, N., and Balch, W. E. (1997) *Science* **277**, 556–558
12. Nufer, O., and Hauri, H. P. (2003) *Curr. Biol.* **13**, R391–393
13. Slack, J. L., Schooley, K., Bonnert, T. P., Mitcham, J. L., Qwarnstrom, E. E., Sims, J. E., and Dower, S. K. (2000) *J. Biol. Chem.* **275**, 4670–4678
14. Latz, E., Visintin, A., Lien, E., Fitzgerald, K. A., Monks, B. G., Kurt-Jones, E. A., Golenbock, D. T., and Espevik, T. (2002) *J. Biol. Chem.* **277**, 47834–47843
15. Nagai, Y., Akashi, S., Nagafuku, M., Ogata, M., Iwakura, Y., Akira, S., Kitamura, T., Kosugi, A., Kimoto, M., and Miyake, K. (2002) *Nat. Immunol.* **3**, 667–672
16. Hein, C., and Andre, B. (1997) *Mol. Microbiol.* **24**, 607–616
17. Beutler, B. (2000) *Curr. Opin. Immunol.* **12**, 20–26
18. Akashi, S., Ogata, H., Kirikae, F., Kirikae, T., Kawasaki, K., Nishijima, M., Shimazu, R., Nagai, Y., Fukudome, K., Kimoto, M., and Miyake, K. (2000) *Biochem. Biophys. Res. Commun.* **268**, 172–177
19. Ohnishi, T., Muroi, M., and Tanamoto, K. (2003) *Clin. Diagn. Lab. Immunol.* **10**, 405–410
20. Xu, Y., Tao, X., Shen, B., Horng, T., Medzhitov, R., Manley, J. L., and Tong, L. (2000) *Nature* **408**, 111–115
21. Dunne, A., Ejdeback, M., Ludidi, P. L., O'Neill, L. A., and Gay, N. J. (2003) *J. Biol. Chem.* **278**, 41443–41451
22. Fitzgerald, K. A., Palsson-McDermott, E. M., Bowie, A. G., Jefferies, C. A., Mansell, A. S., Brady, G., Brint, E., Dunne, A., Gray, P., Harte, M. T., McMurray, D., Smith, D. E., Sims, J. E., Bird, T. A., and O'Neill, L. A. (2001) *Nature* **413**, 78–83
23. Horng, T., Barton, G. M., and Medzhitov, R. (2001) *Nat. Immunol.* **2**, 835–841
24. Schroder, N. W., and Schumann, R. R. (2005) *Lancet Infect. Dis.* **5**, 156–164
25. Agnese, D. M., Calvano, J. E., Hahm, S. J., Coyle, S. M., Corbett, S. A., Calvano, S. E., and Lowry, S. F. (2002) *J. Infect. Dis.* **186**, 1522–1525
26. Randow, F., and Seed, B. (2001) *Nat. Cell Biol.* **3**, 891–896
27. Wakabayashi, Y., Kobayashi, M., Akashi-Takamura, S., Tanimura, N., Konno, K., Takahashi, K., Ishii, T., Mizutani, T., Iba, H., Kouro, T., Takaki, S., Takatsu, K., Oda, Y., Ishihama, Y., Saitoh, S., and Miyake, K. (2006) *J. Immunol.* **177**, 1772–1779
28. Konno, K., Wakabayashi, Y., Akashi-Takamura, S., Ishii, T., Kobayashi, M., Takahashi, K., Kusumoto, Y., Saitoh, S., Yoshizawa, Y., and Miyake, K. (2006) *Biochem. Biophys. Res. Commun.* **339**, 1076–1082
29. Nishitani, C., Mitsuzawa, H., Sano, H., Shimizu, T., Matsushima, N., and Kuroki, Y. (2006) *J. Biol. Chem.* **281**, 38322–38329
30. Akashi, S., Shimazu, R., Ogata, H., Nagai, Y., Takeda, K., Kimoto, M., and Miyake, K. (2000) *J. Immunol.* **164**, 3471–3475
31. Espevik, T., Latz, E., Lien, E., Monks, B., and Golenbock, D. T. (2003) *Scand. J. Infect. Dis.* **35**, 660–664
32. Muta, T., and Takeshige, K. (2001) *Eur. J. Biochem.* **268**, 4580–4589
33. da Silva Correia, J., and Ulevitch, R. J. (2002) *J. Biol. Chem.* **277**, 1845–1854

Atherosclerosis 204 (2009) 619–623

Contents lists available at ScienceDirect

Atherosclerosis

journal homepage: www.elsevier.com/locate/atherosclerosis

Association between metabolic syndrome and carotid atherosclerosis in individuals without diabetes based on the oral glucose tolerance test

Nobukazu Ishizaka[a,*], Yuko Ishizaka[b], Minoru Yamakado[b], Eiichi Toda[b], Kazuhiko Koike[c], Ryozo Nagai[a]

[a] Department of Cardiovascular Medicine, University of Tokyo, Graduate School of Medicine, Hongo 7-3-1 Bunkyo-ku, Tokyo 113-8655, Japan
[b] Center for Multiphasic Health Testing and Services, Mitsui Memorial Hospital, Tokyo, Japan
[c] Department of Infectious Diseases, University of Tokyo, Graduate School of Medicine, Tokyo, Japan

ARTICLE INFO

Article history:
Received 31 July 2008
Received in revised form 20 October 2008
Accepted 21 October 2008
Available online 30 October 2008

Keywords:
Metabolic syndrome
Carotid artery
Atherosclerosis
Risk factors
Glucose metabolism

ABSTRACT

Introduction: Whether or not metabolic syndrome is predictive of atherosclerotic disorders may depend on the population studied. We investigated whether metabolic syndrome is associated with carotid atherosclerosis in individuals who were shown not to have diabetes mellitus based on results of the 75-g oral glucose tolerance test (OGTT).

Methods and results: Between 1994 and 2003, 3904 individuals underwent general health screening that included the OGTT. Among these 3904 individuals, 3679 had a fasting plasma glucose of <126 mg/dL (subgroup 1), and 3488 had a 2-h post-OGTT glucose value of <200 mg/dL (subgroup 2). In both subgroups, metabolic syndrome was found to be a risk factor for carotid plaque and for carotid intima-media thickening in men, and tended to be a risk factor for carotid plaque in women after adjustment for age. Among 3473 individuals who had both a fasting plasma glucose value of <126 mg/dL and a 2-h post-OGTT glucose of <200 mg/dL, 2440 did not have hypertension, which was defined as systolic and diastolic blood pressure of <140/90 mmHg and absence of use of anti-hypertensive medication. In these non-diabetic non-hypertensive individuals, the association between metabolic syndrome and carotid plaque or carotid intima-media thickening was not statistically significant even with adjustment only for age.

Conclusions: In men who did not have impaired fasting glycemia and/or in those without impaired glucose tolerance, metabolic syndrome was a predictor of carotid atherosclerosis after age adjustment, although metabolic syndrome was not found to be a predictor of carotid atherosclerosis when hypertensive individuals were excluded from the study population.

1. Introduction

Metabolic syndrome (MetS) is a cluster of metabolic and hemodynamic abnormalities linked with insulin resistance. Since components of MetS also represent risk factors for atherosclerotic disorders, it is natural that individuals with this syndrome have an increased risk for ischemic heart disease [1] and stroke [2,3]. On the other hand, the clinical utility of MetS may depend on whether the risk conveyed by this syndrome is higher than the sum of each component utilized as diagnostic criteria for MetS [4,5].

Carotid artery intima-media thickness has been reported to be a discriminator as a surrogate of cardiovascular mortality in community-dwelling Japanese people [6] and, conversely, aggregation of established major coronary risk factors has been reported to strongly influence the presence of carotid atherogenesis in the general Japanese population [7]. Previously, we reported that the presence of MetS may not increase the risk for carotid atherosclerosis in individuals without hypertension, with hypertension defined as systolic blood pressure (SBP) of ≥140 mmHg, diastolic blood pressure (DBP) of ≥90 mmHg, or the use of anti-hypertensive medication [8]. This observation suggested that the properties of MetS that present a risk for atherosclerotic diseases may differ according to the populations selected. Consistent with this idea, it was reported that MetS was not found to be associated with cardiovascular mortality in non-diabetic non-hypertensive Chinese individuals [9], and that MetS did not significantly increase the risk of mortality from cardiovascular disease in non-diabetic Mexican Americans and non-Hispanic whites [10]. In the current study, we investigated whether MetS was associated with carotid atherosclerosis in Japanese individuals who did not have diabetes mellitus based on results of the 75-g oral glucose tolerance test (OGTT).

* Corresponding author. Tel.: +81 3 3815 5411x37156; fax: +81 3 5842 5586.
E-mail address: nobuishizka-tky@umin.ac.jp (N. Ishizaka).

0021-9150/$ – see front matter © 2008 Elsevier Ireland Ltd. All rights reserved.
doi:10.1016/j.atherosclerosis.2008.10.022

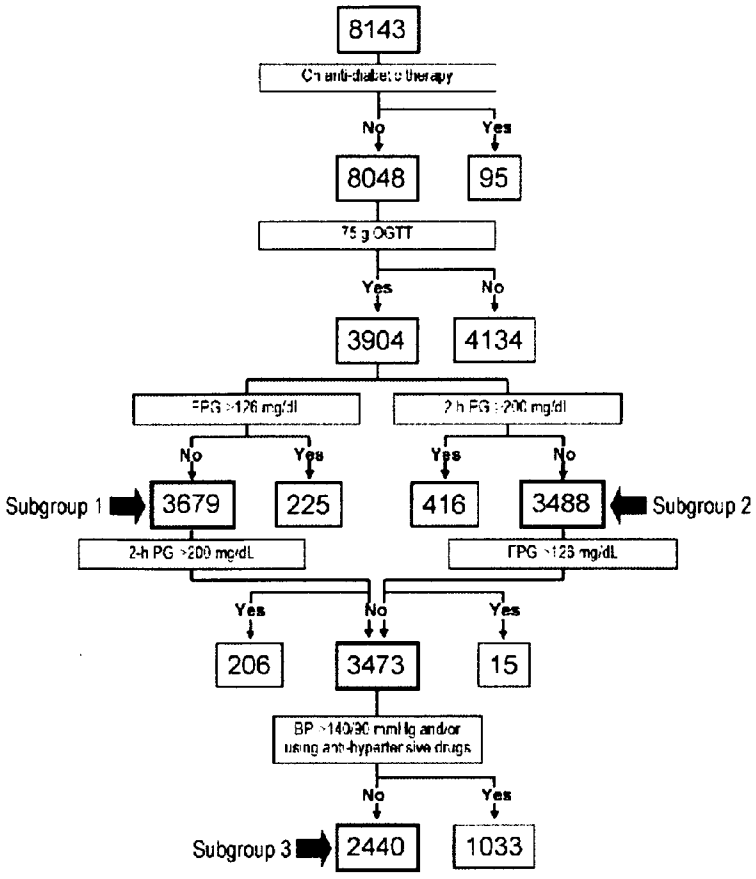

Fig. 1. Flow chart showing selection of the four subgroups.

2. Methods

2.1. Study subjects and selection of subgroups

The study was approved by The Ethical Committee of Mitsui Memorial Hospital and University of Tokyo, Faculty of Medicine. Between September 1994 and December 2003, 8143 subjects underwent general health screening including carotid ultrasonography at the Center for Multiphasic Health Testing and Services, Mitsui Memorial Hospital. Of the 8143 subjects, 95 were treated as having diabetes, and of the remaining 8048 individuals, 3904 underwent an OGTT. Among these 3904 individuals, three subgroups were sequentially selected based on various parameters (Fig. 1). Those with a fasting plasma glucose (FPG) value of <126 mg/dL were designated as subgroup 1, and those with a 2-h post-OGTT plasma glucose (2-h PG) value of <200 mg/dL were designated as subgroup 2. Subgroup 3 was comprised of subjects who met all the following conditions: FPG of <126 mg/dL, 2-h PG of <200 mg/dL, and not having hypertension. Hypertension was defined as SBP ≥140 mmHg, DBP ≥90 mmHg, or the use of antihypertensive medication. We also selected individuals without impaired glucose tolerance (IGT), i.e., individuals with a 2-h PG value of <140 mg/dL.

At our institute, several types of health screening programs are available, and some general health screening programs include carotid ultrasonography and/or OGTT, while others do not. However, the decision on the type of health screening was made by the individuals and/or their companies and was not decided upon or recommended by any attending physician.

2.2. Definition of MetS

MetS was defined as the presence of three or more of the following: (1) fasting glucose ≥110 mg/dL; (2) SBP/DBP ≥130/85 mmHg or taking anti-hypertensive medication; (3) triglycerides ≥150 mg/dL mmol/L; (4) HDL cholesterol <40 mg/dL in men and <50 mg/dL in women; and (5) body mass index ≥25 kg/m^2 [11].

2.3. Carotid ultrasonography

Carotid artery status was studied using high resolution B-mode ultrasonography (Sonolayer SSA270A, Toshiba, Japan) equipped with a 7.5 MHz transducer as described previously [12]. Plaque was defined to be present when there is one or more clearly isolated focal thickening(s) of the intima-media layer with thickness of ≥1.3 mm at the common or internal carotid artery or the carotid bulb. Carotid wall intima-media thickening was said to be present when intima-media thickness which was measured at the far wall of the distal 10 mm of the common carotid artery was ≥1.0 mm [12].

2.4. Statistical analysis

Logistic regression analysis was used to obtain adjusted odds ratios and their 95% confidence intervals (CIs) to predict the presence of carotid plaque or carotid intima-media thickening. Statistical analyses were carried out by using Dr. SPSS II (SPSS Inc., Chicago, IL). Results are expressed as the mean ± standard deviation (SD). A value of $p < 0.05$ was taken to be statistically significant.

Table 1
Baseline characteristics.

Variables	Subgroup 1		Subgroup 2		Subgroup 3	
	Men	Women	Men	Women	Men	Women
Number	2548	1131	2386	1102	1588	852
Age, years	58.2 ± 10.6	57.9 ± 10.4	58.0 ± 10.7	57.8 ± 10.3	56.7 ± 10.9	56.6 ± 10.5
Body mass index, kg/m^2	24.0 ± 2.8	22.2 ± 3.1	23.9 ± 2.7	22.1 ± 3.1	23.6 ± 2.6	21.7 ± 2.8
Systolic BP, mmHg	127 ± 19	121 ± 21	128 ± 19	120 ± 20	119 ± 12	123 ± 14
Diastolic BP, mmHg	79 ± 12	73 ± 12	79 ± 12	73 ± 12	73 ± 8	69 ± 9
Total cholesterol, mg/dL	206 ± 32	219 ± 35	205 ± 32	219 ± 35	205 ± 32	216 ± 35
HDL-cholesterol, mg/dL	55 ± 16	70 ± 17	55 ± 16	70 ± 17	56 ± 16	71 ± 17
Triglycerides, mg/dL	144 ± 117	96 ± 56	142 ± 98	95 ± 54	141 ± 98	95 ± 54
Uric acid, mg/dL	6.2 ± 1.2	4.7 ± 1.0	6.2 ± 1.2	4.7 ± 1.0	6.2 ± 1.2	4.6 ± 1.0
Fasting glucose, mg/dL	96 ± 10	90 ± 10	95 ± 10	90 ± 9	94 ± 9	88 ± 9
2-h OGTT glucose, mg/dL	132 ± 41	118 ± 32	125 ± 29	115 ± 26	121 ± 29	112 ± 25
Haemoglobin A1C, %	5.2 ± 0.4	5.1 ± 0.4	5.2 ± 0.4	5.1 ± 0.4	5.2 ± 0.4	5.1 ± 0.4
Hypertension, *n* (%)	863 (34)	263 (23)	788 (33)	248 (23)	0	0
Anti-hypertensive drugs, *n* (%)	336(13)	99(9)	307(13)	95(9)	0	0
Metabolic syndrome, *n* (%)	439(17)	84(7)	372(16)	72(7)	131 (8)	25(3)
Smoking status						
Never, *n* (%)	764 (30)	933 (82)	714(30)	909 (82)	465 (29)	689(81)
Former, *n* (%)	799(31)	53(5)	753 (32)	50(5)	464 (29)	44(5)
Current, *n* (%)	985 (39)	145(13)	919(39)	143(13)	659(41)	119(14)

BP indicates blood pressure, OGTT indicates oral glucose tolerance test.

3. Results

3.1. Association between MetS and carotid atherosclerosis in individuals with FPG value of <126 mg/dL (subgroup 1)

Among the 3904 individuals who underwent OGTT, 3679 (94%) had an FPG value of less than 126 mg/dL. Of these, 300 (257 men, 43 women), the FPG value was ≥110 mg/dL, thus impaired fasting glycemia (IFG), and in the remaining 3379 (2291 men, 1088 women) had an FPG value of less than 110 mg/dL (no IFG). Table 1 shows the baseline characteristics of this group according to gender. Carotid plaque was found in 823 (32%) men and 191 (17%) women and carotid intima-media thickening was found in 422 (17%) men and 122 (11%) women (Fig. 2). Age-adjusted logistic regression analysis (Model 2) showed that, in men, MetS was statistically significantly associated with carotid plaque (Table 1) and intima-media thickening (Table 2). In women, MetS tended to be associated with carotid plaque, but not with intima-media thickening after age adjustment. Similar patterns of relationships could be observed after further adjustment for total cholesterol (TC) and smoking status (Model 3). On the other hand, after full adjustment including that for components of MetS (Model 4), MetS was not significantly associated with carotid plaque or intima-media thickening in either men or women.

3.2. Association between metabolic syndrome and carotid atherosclerosis in individuals with 2-h PG value of <200 mg/dL (subgroup 2)

Among 3904 individuals who underwent OGTT, 3488 (89%) had a 2-h PG value of less than 200 mg/dL. Of these 3488 individuals 2644 (1717 men, 927 women) had a 2-h PG value of less than 140 mg/dL (no IGT) and the remaining 844 (669 men, 175 women) had a 2-h PG FPG value of ≥140 mg/dL, and thus IGT. Carotid plaque was found in 761 (32%) men and 182 (17%) women and carotid intima-media thickening was found in 378 (16%) men and 116 (11%) women. Age-adjusted logistic regression analysis (Model 2) showed that, in men, MetS was statistically significantly associated with carotid plaque (Table 2) and intima-media thickening (Table 3). In women, MetS tended to be associated with carotid plaque but not with intima-media thickening. Similar patterns of relationship could be observed after further adjustment for TC and smoking status (Model 3). On the other hand, after full adjustment that included components of MetS (Model 4), MetS was not significantly associated with carotid plaque or intima-media thickening in men or in women. There were only 15 (13 men, 2 women)

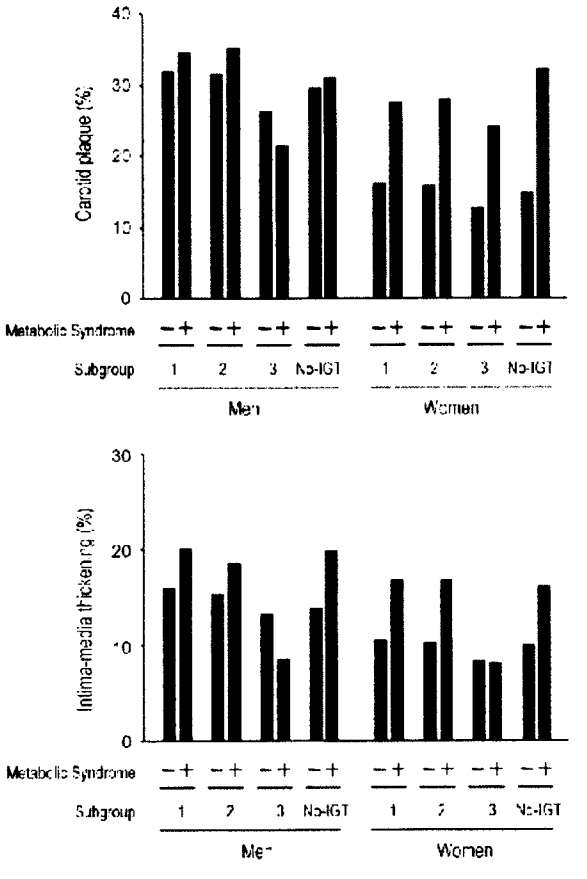

Fig. 2. Prevalence of carotid plaque and carotid intima-media thickening according to the presence or absence of metabolic syndrome in subgroups.

Table 2
Logistic regression analysis with metabolic syndrome as an independent variable and carotid plaque as a dependent variable.

Variables	Odds ratio for carotid plaque			
	Men		Women	
	Odds ratio (95% CI)	*P* value	Odds ratio (95% CI)	*P* value
Subgroup 1				
Model 1	1.12(0.90–1.39)	0.302	1.97(1.19–3.28)	0.009
Model 2	1.41(1.11–1.79)	0.005	1.68(0.96–2.95)	0.072
Model 3	1.30(1.03–1.67)	0.030	1.63(0.93–2.88)	0.091
Model 4	1.21(0.90–1.63)	0.209	1.61(0.79–3.29)	0.188
Subgroup 2				
Model 1	1.18(0.93–1.49)	0.170	2.06(1.20–3.55)	0.009
Model 2	1.47(1.14–1.90)	0.003	1.78(0.98–3.24)	0.058
Model 3	1.38(1.07–1.78)	0.014	1.72(0.95–3.14)	0.076
Model 4	1.23(0.90–1.69)	0.202	1.73(0.82–3.63)	0.151
Subgroup 3				
Model 1	0.77(0.50–1.19)	0.232	2.20(0.86–5.62)	0.101
Model 2	0.99(0.62–1.58)	0.971	1.89(0.66–5.43)	0.235
Model 3	0.94(0.59–1.50)	0.796	1.85(0.64–5.33)	0.254
Model 4	0.82(0.48–1.41)	0.479	2.44(0.72–8.29)	0.152

Model 1, unadjusted; Model 2, adjusted for age; Model 3, adjusted for age, total cholesterol and smoking status; Model 4, adjusted for age, body mass index, systolic blood pressure, total cholesterol, HDL cholesterol, triglycerides, fasting plasma glucose, and smoking status.

individuals among the 3488 in subgroup 2 who had an FPG value of <126 mg/dL in addition to a 2-h PG value of <200 mg/dL, and, thus, the mode of association between MetS, carotid plaque, and intima-media thickening in this subgroup was essentially the same as that observed in total population of subgroup 2.

We also investigated the association between MetS and carotid atherosclerosis in individuals without IGT. There were 2644 individuals who did not have IGT, and among them, 61 had FPG value of ≥110 mg/dL (Fig. 2, Supplementary Tables 1 and 2). The obtained results in these subgroups were similar to those in the subgroup 2; however, association between MetS and carotid intima-media thickening was statistically significant even after multivariate adjustment in women.

Table 3
Logistic regression analysis with metabolic syndrome as an independent variable and carotid intima-media thickening as a dependent variable.

Variables	Odds ratio for carotid intima-media thickening			
	Men		Women	
	Odds ratio (95% CI)	*P* value	Odds ratio (95% CI)	*P* value
Subgroup 1				
Model 1	1.33(1.03–1.73)	0.031	1.74(0.95–3.19)	0.074
Model 2	1.74(1.31–2.30)	<0.001	1.40(0.72–2.73)	0.324
Model 3	1.65(1.24–2.19)	<0.001	1.38(0.70–2.70)	0.349
Model 4	0.97(0.67–1.39)	0.851	0.70(0.31–1.60)	0.398
Subgroup 2				
Model 1	1.26(0.94–1.68)	0.120	1.78(0.93–3.42)	0.083
Model 2	1.63(1.20–2.22)	0.002	1.47(0.73–2.98)	0.285
Model 3	1.55(1.13–2.11)	0.006	1.44(0.71–2.93)	0.317
Model 4	1.00(0.68–1.48)	0.993	0.71(0.30–1.67)	0.435
Subgroup 3				
Model 1	0.61(0.32–1.15)	0.125	0.99(0.23–4.28)	0.985
Model 2	0.83(0.43–1.61)	0.586	0.71(0.15–3.41)	0.673
Model 3	0.77(0.40–1.50)	0.443	0.70(0.15–3.39)	0.660
Model 4	0.52(0.24–1.11)	0.092	0.56(0.05–1.45)	0.123

Model 1, unadjusted; Model 2, adjusted for age; Model 3, adjusted for age, total cholesterol and smoking status; Model 4, adjusted for age, body mass index, systolic blood pressure, total cholesterol, HDL cholesterol, triglycerides, fasting plasma glucose, and smoking status.

3.3. Association between metabolic syndrome and carotid atherosclerosis in individuals with FPG value of <126 mg/dL, 2-h PG value of <200 mg/dL, and no hypertension (subgroup 3)

Among 3904 individuals who underwent OGTT, 2440 (63%) could be assigned to subgroups 3. Their baseline characteristics according to gender are shown in Table 1. Carotid plaque was found in 409 (26%) men and 110 (13%) women and carotid intima-media thickening was found in 202 (13%) men and 69 (8%) women. Unlike subgroups 1 and 2, MetS was not significantly associated with either carotid plaque or intima-media thickening after age adjustment, or even before any adjustment in either gender (Tables 2 and 3).

4. Discussion

Here, we have assessed whether MetS is a risk factor for carotid atherosclerosis in individuals who were determined not to have diabetes mellitus based on results of OGTT. MetS was found to be associated with carotid atherosclerosis especially in men; however, when individuals with hypertension, defined as those having SBP/DBP ≥140/90 mmHg or using anti-hypertensive medication, were excluded, the presence of MetS no longer conferred excess risk when adjustments were made only for age or even when no adjustments were made.

It is known that clustering of certain metabolic abnormalities and hypertension increases the incidence of atherosclerotic diseases [13]. However, whether such clustering of atherogenic risk factors should be separately designated as MetS has been controversial. Whether MetS is independently associated with carotid atherosclerosis has been analyzed in various populations. By analyzing data on a multi-ethnic cohort of apparently healthy individuals in Canada, Paras et al. reported that although MetS was significantly associated with measures of sub-clinical carotid atherosclerosis, this association is mediated entirely through the components of MetS that have been considered as risk factors [14]. Similarly, by analyzing data on individuals recruited from a local community in Italy, Fadini et al. demonstrated that the clustering of MetS components led to a no-more-than additive increase in carotid intima-media thickness [4]. In addition, Vaidya et al. reported that MetS did not have supra-additive association with carotid intima-media thickening [15].

In our previous study that analyzed data on subjects who underwent general health screening, we found that MetS may not be associated with carotid atherosclerosis even after adjustment only for age when individuals did not have hypertension (SBP/DBP <140/90 mmHg and not using anti-hypertensive medication) [8]. In the current study, we expanded this theme to investigate whether MetS increases the risk for carotid atherosclerosis in individuals who had no or only mild (i.e., not in the diabetic range) abnormalities in glucose metabolism. We found that in individuals with FPG values of <126 mg/dL (subgroup 1) or in those with 2-h PG values of <200 mg/dL (subgroup 2), MetS was positively associated with carotid plaque after adjustment for only age (Model 2), although the relationship was only borderline positive in women. In men, the association between MetS and carotid intima-media thickening was also statistically significantly positive after adjustment for only age. These associations lost statistical significance after adjustment for TC, smoking status, and components of MetS (Model 4), suggesting that these associations may not be independent of these factors. Attention should be given to the fact that after excluding individuals with hypertension from the analysis, the association between MetS and carotid plaque or carotid intima-media thickening was no longer statistically significant even after adjustment for only age (subgroup 3), which is in agreement with our previous finding [8].

Several previous cross-sectional and longitudinal studies have investigated whether MetS increases the risk for atherosclerotic diseases in subjects without apparent impairment in glucose metabolism. A prospective population-based study of Finnish men showed that MetS was associated with higher mortality from coronary heart disease in men without impaired fasting glycemia [16]. Wilson et al. reported that MetS was associated with increased risk for cardiovascular disease in those without diabetes [17]. Leoncini et al. reported that MetS was associated with carotid atherosclerosis in non-diabetic hypertensive individuals who attended an outpatient clinic in Italy [18]. Kawamoto et al. analyzed Japanese inpatients and found that MetS increased the risk for carotid intima-media thickening in non-diabetic subjects [19]. Tzou et al. reported that the presence of MetS increased the composite of carotid intima-media thickness of ≥75th percentile of enrolled subjects in non-diabetic young adults [20]. These results support the notion that the presence of MetS will increase the risk for carotid atherosclerosis even in non-diabetic populations; however, caution should be paid in interpreting these results, as these results were not always adjusted for each component of MetS. The present results showed that MetS was associated with carotid plaque and intima-media thickening in men in subgroups 1, and 2 after adjustment for age, TC, and smoking status, although statistically significance would be lost after further adjustment for MetS components.

We found that in the absence of hypertension (subgroup 3), the association between MetS and carotid plaque or intima-media thickening was no more statistically significant after adjustment for only age, or even when no adjustments were made. These data collectively suggested that the presence or absence of hypertension, but not an abnormality in glucose metabolism, is crucial to determine whether the presence of MetS would increase the risk for carotid atherosclerosis. A recent study showed that MetS significantly increased all-cause mortality in hypertensive community-based French individuals with a hazard ratio of 1.40 (95% CI 1.13–1.74), but not in non-hypertensive individuals, during a mean follow-up period of 4.7 years [21], which was consistent with the idea of major role played by hypertension.

This study has several limitations. First, due to the cross-sectional nature of the study, we cannot determine whether there is a causal or resultant relationship between the MetS and presence of atherosclerosis. Second, among 8048 individuals who were not taking anti-diabetic medication, we excluded 4144 individuals who did not undergo OGTT. The mean age of the 3904 individuals who underwent OGTT and those 4144 who did not were significantly different (55 ± 10 years versus 58 ± 10 years, respectively, $P < 0.001$); therefore, it could be said that there had been some selection bias, though, again, the type of health screening was not decided or recommended by the physicians.

In conclusion, we showed that MetS was associated with carotid plaque and carotid intima-media thickening in non-diabetic individuals; although, this relationship did not remain statistically significant after adjustment for MetS components. In non-diabetic non-hypertensive individuals, the association between MetS and carotid plaque or carotid intima-media thickening was not statistically significant when adjustment was made for only age or even when no adjustment were made. These data collectively indicate that presence or absence of hypertension, but not an abnormality in glucose metabolism, is crucial to determine the relationship between MetS and carotid atherosclerosis.

Acknowledgements

The work was supported in part by a grant from the Smoking Research Foundation, that from Chiyoda Mutual Life Foundation, from the St. Luke's Grant for the Epidemiological Research, and that from Daiwa Securities Health Foundation. We are highly appreciative of Kyoko Furuta for her excellent technical assistance.

Appendix A. Supplementary data

Supplementary data associated with this article can be found, in the online version, at doi: 10.1016/j.atherosclerosis.2008.10.022.

References

[1] Iso H, Sato S, Kitamura A, et al. Metabolic syndrome and the risk of ischemic heart disease and stroke among Japanese men and women. Stroke 2007;38:1744–51.
[2] Kwon HM, Kim BJ, Lee SH, Choi SH, Oh BH, Yoon BW. Metabolic syndrome as an independent risk factor of silent brain infarction in healthy people. Stroke 2006;37:466–70.
[3] Wang J, Ruotsalainen S, Moilanen L, Lepisto P, Laakso M, Kuusisto J. The metabolic syndrome predicts incident stroke: a 14-year follow-up study in elderly people in Finland. Stroke 2008;39:1078–83.
[4] Fadini GP, Coracina A, Inchiostro S, Tiengo A, Avogaro A, de Kreutzenberg SV. A stepwise approach to assess the impact of clustering cardiometabolic risk factors on carotid intima-media thickness: the metabolic syndrome no-more-than-additive. Eur J Cardiovasc Prev Rehabil 2008;15:190–6.
[5] Kahn R, Buse J, Ferrannini E, Stern M. The metabolic syndrome: time for a critical appraisal: joint statement from the American Diabetes Association and the European Association for the Study of Diabetes. Diabetes Care 2005;28:2289–304.
[6] Murakami S, Otsuka K, Hotta N, et al. Common carotid intima-media thickness is predictive of all-cause and cardiovascular mortality in elderly community-dwelling people: Longitudinal Investigation for the Longevity and Aging in Hokkaido County (LILAC) study. Biomed Pharmacother 2005;59(Suppl 1):S49–53.
[7] Mannami T, Baba S, Ogata J. Strong and significant relationships between aggregation of major coronary risk factors and the acceleration of carotid atherosclerosis in the general population of a Japanese city: the Suita Study. Arch Intern Med 2000;160:2297–303.
[8] Ishizaka N, Ishizaka Y, Hashimoto H, et al. Metabolic syndrome may not associate with carotid plaque in subjects with optimal, normal, or high-normal blood pressure. Hypertension 2006;48:411–7.
[9] Hsu PF, Chuang SY, Cheng HM, et al. Clinical significance of the metabolic syndrome in the absence of established hypertension and diabetes: a community-based study. Diabetes Res Clin Pract 2008;79:461–7.
[10] Stern MP, Williams K, Hunt KJ. Impact of diabetes/metabolic syndrome in patients with established cardiovascular disease. Atheroscler Suppl 2005;6:3–6.
[11] Ishizaka N, Ishizaka Y, Toda E, Hashimoto H, Nagai R, Yamakado M. Association between cigarette smoking, metabolic syndrome, and carotid arteriosclerosis in Japanese individuals. Atherosclerosis 2005;181:381–8.
[12] Ishizaka N, Ishizaka Y, Takahashi E, et al. Association between insulin resistance and carotid arteriosclerosis in subjects with normal fasting glucose and normal glucose tolerance. Arterioscler Thromb Vasc Biol 2003;23:295–301.
[13] Fowkes FG, Murray GD, Butcher I, et al. Ankle brachial index combined with Framingham Risk Score to predict cardiovascular events and mortality: a meta-analysis. JAMA 2008;300:197–208.
[14] Paras E, Mancini GB, Lear SA. The relationship of three common definitions of the metabolic syndrome with sub-clinical carotid atherosclerosis. Atherosclerosis 2008;198:228–36.
[15] Vaidya D, Szklo M, Liu K, et al. Defining the metabolic syndrome construct: Multi-Ethnic Study of Atherosclerosis (MESA) cross-sectional analysis. Diabetes Care 2007;30:2086–90.
[16] Lakka HM, Laaksonen DE, Lakka TA, et al. The metabolic syndrome and total and cardiovascular disease mortality in middle-aged men. JAMA 2002;288:2709–16.
[17] Wilson PW, D'Agostino RB, Parise H, Sullivan L, Meigs JB. Metabolic syndrome as a precursor of cardiovascular disease and type 2 diabetes mellitus. Circulation 2005;112:3066–72.
[18] Leoncini G, Ratto E, Viazzi F, et al. Metabolic syndrome is associated with early signs of organ damage in nondiabetic, hypertensive patients. J Intern Med 2005;257:454–60.
[19] Kawamoto R, Tomita H, Ohtsuka N, Inoue A, Kamitani A. Metabolic syndrome, diabetes and subclinical atherosclerosis as assessed by carotid intima-media thickness. J Atheroscler Thromb 2007;14:78–85.
[20] Tzou WS, Douglas PS, Srinivasan SR, et al. Increased subclinical atherosclerosis in young adults with metabolic syndrome: the Bogalusa Heart Study. J Am Coll Cardiol 2005;46:457–63.
[21] Pannier B, Thomas F, Bean K, et al. The metabolic syndrome: similar deleterious impact on all-cause mortality in hypertensive and normotensive subjects. J Hypertens 2008;26:1223–8.

J Gastroenterol 2009; 44[Suppl XIX]:82–88
DOI 10.1007/s00535-008-2276-4

Journal of
Gastroenterology

Steatosis, liver injury, and hepatocarcinogenesis in hepatitis C viral infection

KAZUHIKO KOIKE

Department of Infectious Diseases, Internal Medicine, Graduate School of Medicine, University of Tokyo, 7-3-1 Hongo, Bunkyo-ku, Tokyo 113-8655, Japan

In addition to the link with development of hepatocellular carcinoma (HCC), hepatitis C virus (HCV) infection is associated with several hepatic and extrahepatic manifestations. A role of hepatic steatosis in the pathogenesis of chronic hepatitis C has been shown, implying hepatitis C as a metabolic disease. Furthermore, recent epidemiological studies have suggested a linkage between insulin resistance and chronic HCV infection. In addition to the data indicating the presence of lipid metabolism disturbance and insulin resistance in the cohort of chronic hepatitis C patients, we found evidence showing the association between these two conditions and HCV infection using mice transgenic for the HCV core gene. These mice develop HCC late in life after the phase of hepatic steatosis and insulin resistance. The nonappearance of both steatosis and HCC in HCV core gene transgenic mice that are null for the proteasome activator 28γ implies a close relationship between lipid metabolism disturbance and hepatocarcinogenesis. Also, the core protein is shown to bind with retinoid X receptor (RXR)-α, resulting in the upregulation of some lipid metabolism enzymes, including cellular retinol binding protein II and acyl-CoA oxidase. In addition, the persistent activation of peroxisome proliferator activated receptor (PPAR)-α has recently been found in the liver of HCV core gene transgenic mice, yielding dramatic changes in lipid metabolism and hepatocyte proliferation, including HCC development. These results would provide a clue for further understanding of the role of lipid metabolism in pathogenesis of HCV infection, including liver injury and hepatocarcinogenesis.

Received: June 9, 2008 / Accepted: August 10, 2008
Reprint requests to: K. Koike

Key words: lipid metabolism, transgenic mouse, oxidative stress, intracellular signal transduction, peroxisome proliferator activated receptor

Introduction

Worldwide, approximately 170 million people are persistently infected with hepatitis C virus (HCV), which induces a spectrum of chronic liver diseases from chronic hepatitis to cirrhosis and, eventually, to hepatocellular carcinoma (HCC).[1] HCV has been given increasing attention because of its wide and deep penetration in the community, tied with a very high incidence of HCC in persistent HCV infection. Once liver cirrhosis is established in hosts persistently infected with HCV, HCC develops at a yearly rate of approximately 7%,[2] resulting in the development of HCC in nearly 90% of HCV-associated cirrhotic patients in 15 years. In addition, the outstanding features in the mode of hepatocarcinogenesis in HCV infection, i.e., development of HCC in a multicentric fashion and at a very high incidence, are not common in other malignancies except for hereditary cancers such as familial polyposis of the colon. Knowledge of the mechanism underlying HCC development in persistent HCV infection, therefore, is imminently required for the prevention of HCC.

In addition to the link with development of HCC, HCV infection is associated with several hepatic and extrahepatic manifestations.[3] A role of hepatic steatosis in the pathogenesis of chronic hepatitis C has been shown, implicating hepatitis C as a metabolic disease.[4] Moreover, recent epidemiological studies have suggested a linkage between insulin resistance and chronic HCV infection.[5] In addition to the epidemiological data indicating the presence of lipid metabolism disturbance and insulin resistance in the cohort of chronic hepatitis C patients, detailed analyses on the relationship between

metabolic disorders and chronic hepatitis C have revealed evidence showing a close association between the progression of liver fibrosis and metabolic abnormalities in HCV infection.[6] However, it is unclear yet whether a causative relationship exists between these medical conditions. Moreover, it is unclear whether such metabolic disorders contribute to hepatocarcinogenesis in HCV infection.

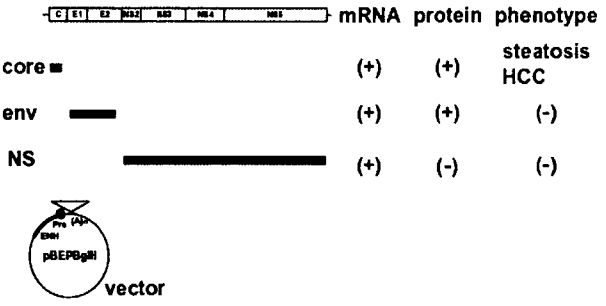

Fig. 1. Transgenic mouse lines carrying the hepatitis C virus (HCV) genome. Three different kinds of transgenic mouse lines, carrying the *core* gene, envelope genes, or nonstructural genes of HCV, respectively, were established under the control of the same regulatory elements. Among these mouse strains, only the transgenic mice carrying the HCV core gene develop hepatocellular carcinoma (HCC) after an early phase with hepatic steatosis in two independent lineages. The mice transgenic for the envelope genes or nonstructural genes do not develop HCC. *HCC*, hepatocellular carcinoma; *env*, envelope genes; *NS*, nonstructural genes

Possible roles of HCV in hepatocarcinogenesis

The mechanism underlying hepatocarcinogenesis in HCV infection is not yet fully understood, despite the fact that nearly 80% of patients with HCC in Japan are persistently infected with HCV.[1,7,8] HCV infection is also common in patients with HCC in other countries, albeit to a lesser extent. These lines of evidence prompted us to seek to determine the role of HCV in hepatocarcinogenesis. Inflammation induced by HCV should be considered, of course, in a study on the hepatocarcinogenesis in hepatitis viral infection: necrosis of hepatocytes caused by chronic inflammation followed by regeneration enhances genetic aberrations in host cells, the accumulation of which culminates in HCC. This theory presupposes an indirect involvement of hepatitis viruses in HCC via hepatic inflammation. However, this context leaves us with a serious question: can inflammation alone result in the development of HCC in such a high incidence (90% in 15 years) or multicentric nature in HCV infection?

The other role of HCV would have to be weighed against an extremely rare occurrence of HCC in patients with autoimmune hepatitis in which severe inflammation in the liver persists indefinitely, even after the development of cirrhosis. This background and reasoning lead to a possible activity of viral proteins for inducing neoplasia. This possibility has been evaluated by introducing genes of HCV into hepatocytes in culture with little success. One of the difficulties in using cultured cells is the carcinogenic capacity of HCV, if any, which would be weak and would take a long time to manifest. Actually, it takes 30–40 years for HCC to develop in individuals infected with HCV. On the basis of these points of view, we started to investigate carcinogenesis in chronic hepatitis C, in vivo, by transgenic mouse technology.

HCV core protein has an in vivo oncogenic activity as revealed by animal studies

Transgenic mouse lines carrying the HCV genome were engineered by introducing the genes from the cDNA of the HCV genome of genotype 1b.[9,10] Established are three different kinds of transgenic mouse lines, which carry the core gene, envelope genes, or nonstructural genes, respectively, under the same transcriptional regulatory element. Among these mouse lines, only the transgenic mice carrying the core gene developed HCC in two independent lineages.[10] The envelope gene transgenic mice do not develop HCC, despite high expression levels of both E1 and E2 proteins,[11,12] and the transgenic mice carrying the entire nonstructural genes have developed no HCC (Fig. 1).

The core gene transgenic mice express the core protein of an expected size, and the level of the core protein in the liver is similar to that in chronic hepatitis C patients. Early in life, these mice develop hepatic steatosis, which is one of the histological characteristics of chronic hepatitis C, along with lymphoid follicle formation and bile duct damage.[13] Thus, the core gene transgenic mouse model reproduces well the features of chronic hepatitis C. Of note, no pictures of significant inflammation are observed in the liver of this animal model. Late in life, these transgenic mice develop HCC. Notably, the development of steatosis and HCC has been reproduced by other HCV transgenic mouse lines, which harbor the entire HCV genome or structural genes including the core gene.[14–16] These outcomes indicate that the core protein, per se, of HCV has an oncogenic potential when expressed in vivo.

Oxidative stress overproduction and intracellular signaling pathway activation are the major pathways in the core-induced liver pathology

It is difficult to elucidate the mechanism underlying the development of HCC, even for our simple model in which only the core protein is expressed in otherwise normal liver. There is a notable feature in the localization of the core protein in hepatocytes; while the core protein predominantly exists in the cytoplasm associated with lipid droplets, it is also present in the mitochondria and nuclei.[10,17] On the basis of this finding, the pathways related to these two organelles, the mitochondria and nuclei, were thoroughly investigated.

One effect of the core protein is an increased production of oxidative stress in the liver. We would like to draw particular attention to the fact that the production of oxidative stress is increased in our transgenic mouse model in the absence of inflammation in the liver. This finding reflects a state of overproduction of reactive oxygen species (ROS) in the liver,[18] or predisposition to it, which is staged by the HCV core protein without any intervening inflammation.[19,20] The overproduction of oxidative stress results in the generation of deletions in mitochondrial and nuclear DNA, an indicator of genetic damage. In addition, analysis of antioxidant system revealed that some antioxidative molecules are not increased despite the overproduction of ROS in the liver of core gene transgenic mice: hemeoxygenase-1 and glutathione peroxidase are not augmented whereas catalase and glutathione S-transferase levels are increased and enhanced by iron overloading (Moriya et al., manuscript in preparation). These results suggest that HCV core protein not only induces overproduction of ROS but also attenuates some of the antioxidant systems, which may explain the mechanism underlying the production of a strong oxidative stress in HCV infection compared to other forms of hepatitis.

In the absence of inflammation, thus, the core protein induces oxidative stress overproduction, which may, at least in part, contribute to hepatocarcinogenesis in HCV infection. If inflammation were added to the liver with the HCV core protein, the production of oxidative stress would be escalated to an extent that can no longer be scavenged by a physiological antagonistic system. This idea suggests that the inflammation in chronic HCV infection would have a characteristic difference in its quality from those of other types of hepatitis, such as autoimmune hepatitis. The basis for the overproduction of oxidative stress may be ascribed to the mitochondrial dysfunction.[10,19] The dysfunction of the electron transfer system of the mitochondrion is suggested in association with the presence of the HCV core protein.[21]

Other pathways in hepatocarcinogenesis would be the alteration of the expression of cellular genes and modulation of intracellular signaling pathways. For example, tumor necrosis factor (TNF)-α and interleukin-1β have been found to be transcriptionally activated.[22] The mitogen-activated protein kinase (MAPK) cascade is also activated in the liver of the core gene transgenic mouse model. The MAPK pathway, which consists of three routes, c-Jun N-terminal kinase (JNK), p38, and extracellular signal-regulated kinase (ERK), is involved in numerous cellular events including cell proliferation. In the liver of the core gene transgenic mouse model before HCC development, only the JNK route is activated. Downstream of JNK activation, transcription factor activating protein (AP)-1 activation is markedly enhanced.[20,21] At far downstream, both the mRNA and protein levels of cyclin D1 and CDK4 are increased. Thus, the HCV core protein modulates the intracellular signaling pathways and gives an advantage for cell proliferation to the hepatocytes. Interestingly, we found recently that a protein interacting with the core protein, proteasome activator 28γ (PA28γ), is indispensable for the core protein to exert its function for the development of steatosis, insulin resistance, and HCC.[23,24]

Lipid metabolism and HCV infection

Steatosis is frequently observed in chronic hepatitis C patients and is significantly associated with increased fibrosis and progression rate of fibrosis of the liver.[6] A comprehensive analysis of gene expression in the liver of core gene transgenic mice, in which steatosis develops from early in life, revealed that a number of genes related to lipid metabolism are significantly upregulated or downregulated (Table 1).

The composition of fatty acids that are accumulated in the liver of core gene transgenic mice is different from that in fatty liver resulting from simple obesity. Carbon-18 monounsaturated fatty acids (C18:1) such as oleic or vaccenic acids are significantly increased; this is also the case in the comparison of liver tissues from hepatitis C patients and patients with simple fatty liver due to obesity.[20] The mechanism of steatogenesis in hepatitis C was investigated using this mouse model. There are at least three pathways for the development of steatosis. One is the frequent presence of insulin resistance in hepatitis C patients as well as in the core gene transgenic mice, which occurs through the inhibition of tyrosine phosphorylation of insulin receptor substrate (IRS)-1.[25] Insulin resistance increases the peripheral release and hepatic uptake of fatty acids, resulting in an accumulation of lipid in the liver. The second pathway is the suppression of the activity of